energies

MDPI

Article

Multi-Input Modeling Approach to Assess the Impacts of Climate Change on Grand Inga Hydropower Potential

Salomon Salumu Zahera [1,2,*], Ånund Killingtveit [3] and Musandji Fuamba [1]

[1] École Polytechnique, Montreal, QC H3T 0A3, Canada; musandji.fuamba@polymtl.ca
[2] Institut National du Bâtiment et des Travaux-Publics, Kinshasa B.P. 4731, Democratic Republic of the Congo
[3] Department of Civil and Environmental Engineering, Faculty of Engineering, Norwegian University of Science and Technology—NTNU, 7491 Trondheim, Norway; anund.killingtveit@ntnu.no
* Correspondence: salomon.salumu@polymtl.ca; Tel.: +1-514-839-4030

Abstract: This study assesses the potential impact of climate change on hydropower generation, focusing on the Grand Inga hydropower project on the Congo River in the Democratic Republic of Congo. Utilizing a multi-input approach with a conceptual HEC-HMS hydrologic model, this research incorporates a new bias-corrected high-resolution daily downscaled dataset, NASA Earth Exchange Global Daily Downscaled Projections (NEX-GDDP CMIP6), and its predecessor (CMIP5) under various climate scenarios. The hydropower generation at Inga Falls is simulated using a hydropower model, considering observed and simulated daily flows for different climate models and emission scenarios. The results suggest that the Grand Inga project will be resilient to negative climate impacts during its initial phases (1–5). The system demonstrates security and insensitivity to adverse changes, both for existing (Phase 1–2) and planned (Phase 3–5) hydropower components. This study indicates that climate change effects become apparent only in later phases (6–8), with predominantly positive impacts, potentially increasing the generation potential of the hydropower system. Overall, the Grand Inga hydropower project appears robust against adverse climate influences throughout the majority of its development phases.

Keywords: Grand Inga; multi-input approach; Granger Ramanathan C averaging; NASA Earth Exchange Global Daily Downscaled Projections Datasets; Congo Basin

Academic Editors: Sue Ellen Haupt, Alberto Troccoli and Laurent Dubus

Received: 17 November 2024
Revised: 2 March 2025
Accepted: 7 March 2025
Published: 3 April 2025

Citation: Salumu Zahera, S.; Killingtveit, Å.; Fuamba, M. Multi-Input Modeling Approach to Assess the Impacts of Climate Change on Grand Inga Hydropower Potential. *Energies* **2025**, *18*, 1819. https://doi.org/10.3390/en18071819

1. Introduction

The acceleration of the global water cycle through increased evaporation and precipitation rates caused by greenhouse gas (GHG) emissions is a direct consequence of climate change [1–3]. This alteration redistributes water resources and intensifies the frequency and severity of extreme hydrological events [1,3,4], thereby impacting the operation of water infrastructure such as dam design and hydropower production [1,5–8].

The growing energy demand to support socioeconomic advancement is anticipated to drive further GHG emissions, amplifying atmospheric concentrations and resulting in a more pronounced climate and hydrological shift in the 21st century [9]. Against this backdrop, hydropower emerges as a dominant and cost-effective renewable energy source that plays a pivotal role in curbing GHG emissions and mitigating climate change. It is experiencing robust expansion across various global regions [10–13].

Previous studies have predominantly explored climate change's impact on water resources and hydropower generation using a top-down modeling approach. These studies integrated projections from general circulation models (GCMs) with hydrological models, reservoir operation models, and hydropower models [14–18]. It was generally observed

that globally, projected annual mean streamflow would rise in high-latitude and wet tropical areas, while it would decrease in most dry tropical regions, alongside increased frequency of hydrological extremes [1,9].

Climate change introduces variability in precipitation and temperature patterns, impacting the streamflow regime and consequently affecting the resource potential of a basin [19–21]. Given that hydrological inputs are pivotal in assessing hydropower system potential, climate change impact assessments (CCIA) should integrate hydrologic models that accurately represent the contributing catchment [22–25]. These studies inherently carry uncertainties [25], primarily stemming from climate model and emission scenario uncertainties. To mitigate this, ensemble-based studies are recommended [21,26,27], with hydrologic model-based climate change assessments incorporating climate model ensembles [28,29].

Climate change studies utilize a variety of climate models to simulate future scenarios based on different greenhouse gas emission pathways. Projected climate variable data can be derived from various simulation runs of climate models, with general circulation models (GCMs) being common. Regional climate models (RCMs) offer a solution by providing high-resolution climate information based on GCM data [30–32].

The National Aeronautics and Space Administration (NASA) recently launched the Earth Exchange Global Daily Downscaled Projections (NEXGDDP) dataset, which facilitates future climate change studies at the watershed scale, as demonstrated by [33,34].

The Grand Inga hydropower project (GIHP) on the Congo River in the Democratic Republic of Congo (DRC) is a notable initiative, comprising the world's largest proposed hydropower scheme. Positioned at the Inga Falls site, it holds enormous potential for energy production. As climate change poses a significant threat to such projects, evaluating its impact on hydropower generation becomes imperative.

Thus, this study focuses on the specific challenges and opportunities posed by climate change for the Grand Inga hydropower project, unlike previous studies that explored broader impacts on water resources and hydropower generation. By narrowing its scope, the study provides a detailed and comprehensive analysis tailored to the world's largest proposed hydropower scheme.

Leveraging the Earth Exchange Global Daily Downscaled Projections (NEXGDDP) dataset by NASA, this study utilizes high-resolution climate information at the watershed scale. This approach offers a more granular and accurate assessment of climate change's impact on GIHP performance compared to previous studies that relied on less detailed climate data.

Additionally, to address uncertainties in climate modeling, this study adopts an ensemble-based approach. By integrating multiple climate models and scenarios, it enhances the robustness and reliability of its projections, providing nuanced insights into future hydrology and energy generation scenarios for GIHP.

2. Grand Inga—Overview and Project Planning

2.1. Overview on Inga Falls

The hydropower potential of the Congo River at the Inga site has been recognized since the early 20th century. Located approximately 280 km downstream of Kinshasa, the capital of the Democratic Republic of the Congo (DRC), the Inga site spans a 32-km stretch of river with a natural elevation drop of 97 m. With a mean annual flow (MAF) of approximately 40,000 m^3/s and a gross head that can be increased to 150 m, the hydroelectric potential at Inga Falls is immense. This site has the capacity to exceed 47,000 MW of installed power, with an annual generation surpassing 360 TWh—significantly greater than Africa's total hydropower capacity in 2021, which stood at 38,000 MW and 146 TWh.

The first two phases of development at the Inga site, Inga 1 (350 MW) and Inga 2 (1400 MW), were completed in 1971 and 1982, respectively. However, since then, no major new hydropower plants have been constructed in the country, leaving the vast potential of the site largely untapped.

2.2. Development Prospects of Grand Inga

Many studies on further development of Grand Inga have been performed. A good summary of possible future development is given by Nzakimuena, St-Pierre and Zahera and Fuamba [35,36]. The hydropower simulation models developed in this study are based on the final proposed scheme designed by the AECOM-RSW/EDF consortium and submitted to the Congolese government in 2012 as part of the provisional feasibility report for the development of the Inga hydroelectric site and its associated interconnections. In this scheme, further development has been planned in several phases, from Phase 3 to Phase 8. Each phase will consist of several turbine/generator sets, from eight to twelve in each. Figure 1 situates the Inga site within the Congo Basin.

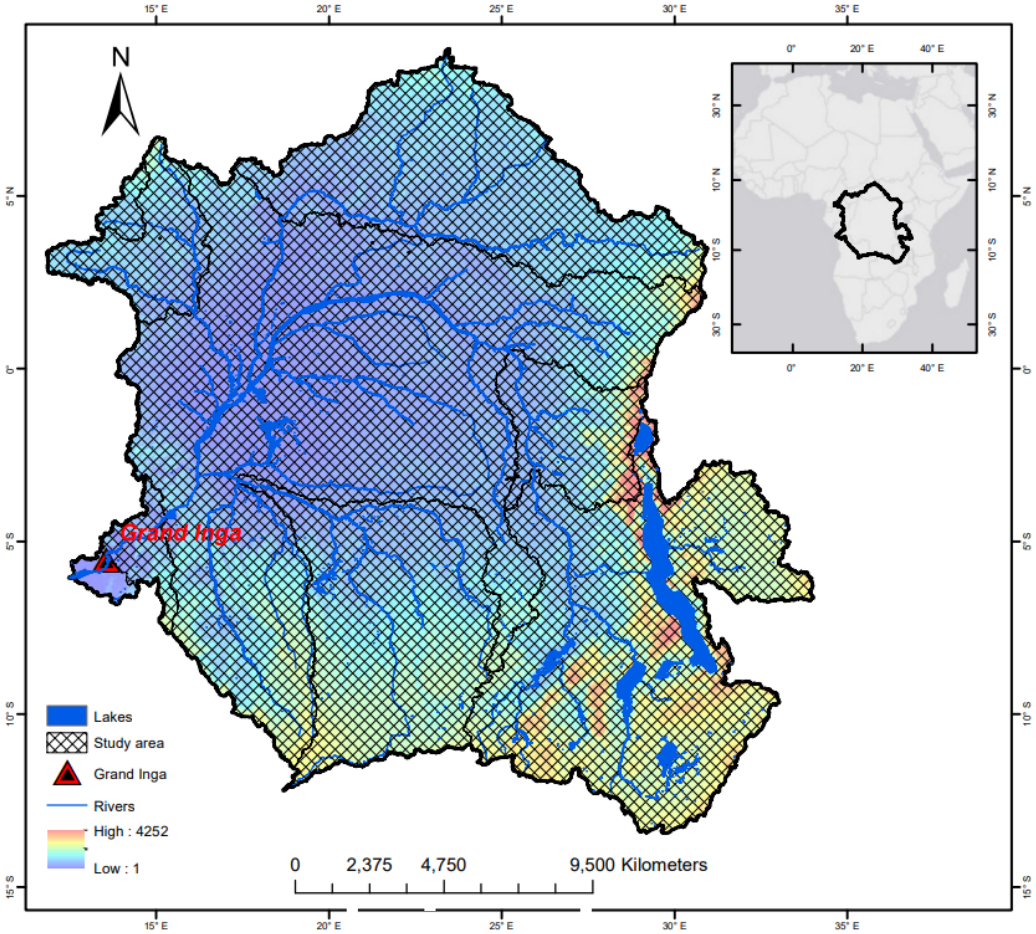

Figure 1. Congo River Basin at the Inga outlet.

3. Data and Methods

3.1. Modelling Procedure

This study began with the development of a conceptual hydrological model, calibrated using historical climate data and observed streamflow records. The hydrological model is then driven by the projected high-resolution NASA Earth Exchange Global Daily Downscaled Projections (NEX-GDDP) dataset. The hydropower generation model is subsequently applied to estimate future energy production.

3.2. Data

3.2.1. System Data for Inga Falls Hydropower Development

Data for existing (Inga 1 and 2) and planned (Inga 3–8) phases is summarized in Tables 1 and 2 summarizes the cumulative values of flow and capacity for each phase. It should be noted that further development is also possible, given that a residual fall still exists after the installation of the eight projected phases. Some calculations are performed here for two additional phases (Inga 9 and 10).

Table 1. Main technical data for the Inga Falls hydropower system (Source: Nzakimuena et al., 2013 [34]).

Main Steps (Phases) in Inga's Development		Data per Unit (Turbine/Generator)				
Phase	**# of Units**	**Q_{max} [m^3/s]**	**Head [m]**	**EEQV1 [KWh/m^3]**	**EEQV2 [$MW/m^3/s$]**	**P_{max} [MW]**
Inga 1	6	130	50	0.125	0.450	58.5
Inga 2	8	252.5	58	0.157	0.566	143
Inga 3	11	600	150	0.376	1.354	813
Inga 4	8	685	150	0.376	1.354	928
Inga 5	8	685	150	0.376	1.354	928
Inga 6	8	685	150	0.376	1.354	928
Inga 7	8	685	150	0.376	1.354	928
Inga 8	8	685	150	0.376	1.354	928
Inga 9	8	685	150	0.376	1.354	928
Inga 10	8	685	150	0.376	1.354	928
Rest	1					

Table 2. Cumulative values of flow and capacity for each phase.

Cumulative Values		
	Q_{max}	**P_{max}**
Phase	**m^3/s**	**MW**
Inga 1	780	351
Inga 2	2800	1495
Inga 3	9400	10,434
Inga 4	14,880	17,856
Inga 5	20,360	25,278
Inga 6	25,840	32,700
Inga 7	31,320	40,122
Inga 8	36,800	47,544

Q_{max}: max turbine flow. Head: gross head intake to tailwater. EEQV1: energy equivalent of water, KWh/m^3. EEQV2: power equivalent of water, MW per m^3/s. P_{max}: power capacity at full turbine flow, MW. The three columns, EEQV1, EEQV2, and P_{max}, have been computed based on Q_{max} and Head, with additional assumptions regarding turbine and generator efficiency, as well as head losses. Phase 9 and 10 have been added here to show the possibility of further expansion of the project and compute utilization. Same type of turbines as in Inga 4–8 have been assumed.

3.2.2. System Data

The streamflow data for the Inga outlet were obtained from the Régie des Voies Fluviales (R.V.F). These data were essential for calibrating the hydrological model and evaluating its performance. The dataset includes daily flow rates at Inga Falls over a 20-year period, from 1 January 1981 to 30 December 2000 (Figure 2a). The corresponding flow duration curve is presented in Figure 2b.

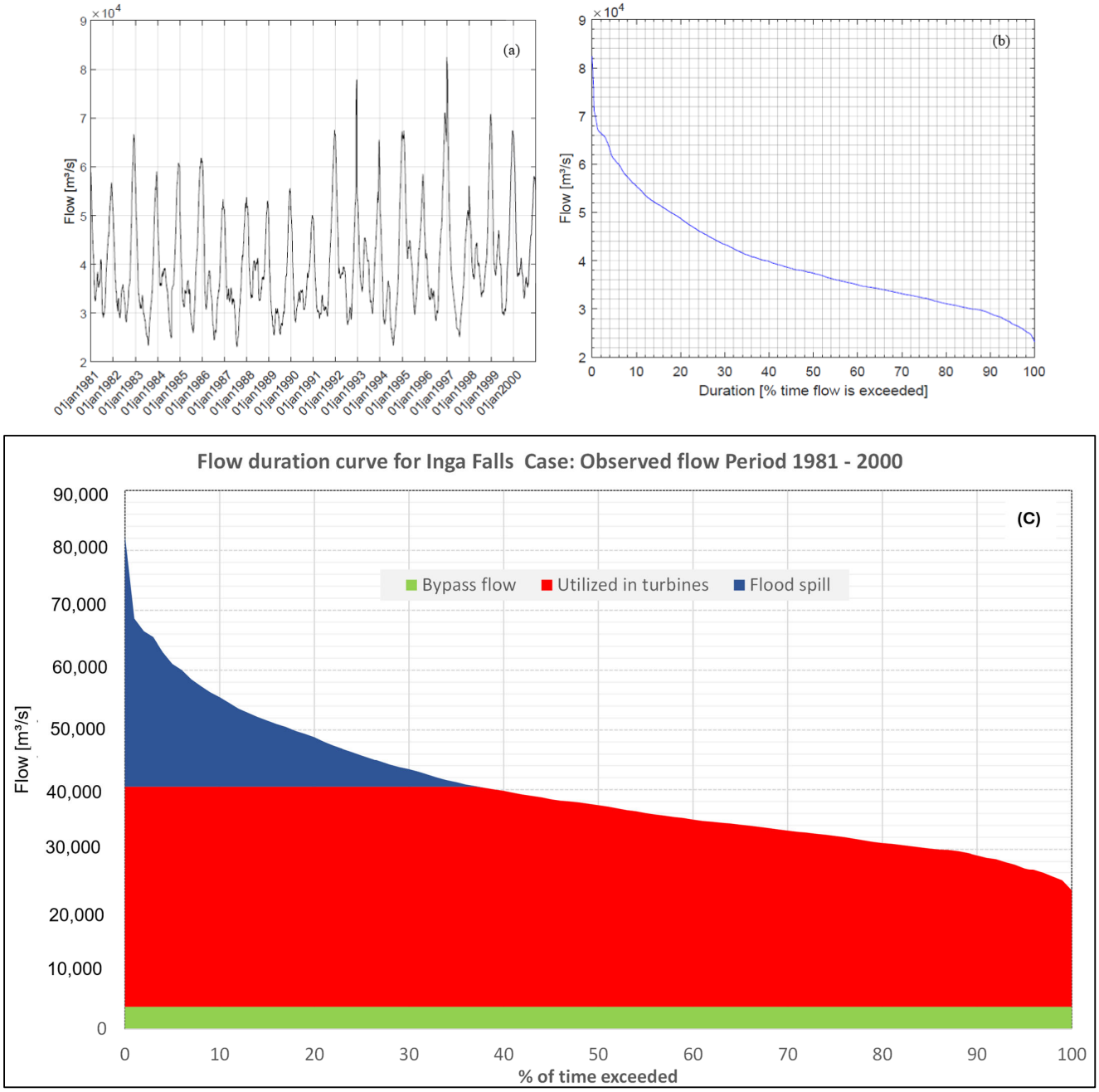

Figure 2. (**a**) Daily water flow, (**b**) flow duration curve at Inga Falls, and (**c**) water utilization duration curve for Inga Falls with full development.

Key statistics extracted from the dataset are as follows:
Average flow: 39,912 m^3/s
Median flow: 37,393 m^3/s
Maximum flow: 82,428 m^3/s (occurred on 28 December 1996)
Minimum flow: 23,063 m^3/s (recorded on 26 July 1987)

3.2.3. Future Climate Projection Data

To evaluate the hydrological response to climate change in the Congo River Basin, this study utilized the high-resolution NASA Earth Exchange Global Daily Downscaled Projections (NEX-GDDP) dataset.

The NEX-GDDP-CMIP5 [37] and NEX-GDDP-CMIP6 [38] datasets are valuable resources for studying the impacts of climate change at the scale of individual towns, cities,

and watersheds. These datasets provide high-resolution (0.25° × 0.25°) downscaled outputs from the Coupled Model Intercomparison Project Phase 5 (CMIP5) and Phase 6 (CMIP6) global climate models (GCMs). Available as daily projections spanning from 1950 to 2100, they offer detailed insights for localized climate analysis.

To enhance the performance of low-resolution GCMs and correct local biases, the bias correction and spatial disaggregation (BCSD) regression-based statistical downscaling method was applied in developing this dataset [37–39]. This study selected a subset of 13 CMIP6 models along with their CMIP5 predecessors (Table 3).

Table 3. Overview of 13 NEX-GDDP CMIP6 models and their predecessors CMIP5 used in this study.

Model Name		Modeling Agency	Resolution Lon. × Lat.
CMIP6	**CMIP5**		
BCC-CSM2-MR	BNU-ESM	Beijing Climate Center, China Meteorological Administration (China)	0.25° × 0.25°
CanESM5	CanESM2	Canadian Centre for Climate Modelling and Analysis (Canada)	0.25° × 0.25°
CNRM-CM6-1	CNRM-CM5	Centre National de Recherches Météorologiques, France	0.25° × 0.25°
GFDL-CM4-gr2	GFDL-ESM2G	Geophysical Fluid Dynamics Laboratory, USA	0.25° × 0.25°
GFDL-ESM4	GFDL-ESM2M	Geophysical Fluid Dynamics Laboratory, USA	0.25° × 0.25°
INM-CM5-0	INM-CM4	Institute for Numerical Mathematics, Russian Academy of Science/Russia	0.25° × 0.25°
IPSL-CM6A-LR	IPSL-CM5A-LR	L'Institut Pierre-Simon Laplace (France)	0.25° × 0.25°
MIROC6	MIROC-ESM	National Institute for Environmental Studies, The University of Tokyo (Japan)	0.25° × 0.25°
MIROC-ES2L	MIROC-ESM-CHEM	National Institute for Environmental Studies, The University of Tokyo (Japan)	0.25° × 0.25°
MPI-ESM-1-2-HR	MPI-ESM-MR	Max Planck Institute for Meteorology (Germany)	0.25° × 0.25°
MPI-ESM-1-2-LR	MPI-ESM-LR	Max Planck Institute for Meteorology (Germany)	0.25° × 0.25°
MRI-ESM2-0	MRI-CGCM3	Meteorological Research Institute (Japan)	0.25° × 0.25°
NorESM2-LM	NorESM1-M	Norwegian Climate Centre (Norway)	0.25° × 0.25°

3.2.4. Differences and Connections Between CMIP6 and CMIP5

The Coupled Model Intercomparison Project (CMIP) is a coordinated effort to improve climate projections and understanding by running standardized climate model experiments. CMIP6 builds upon CMIP5, with significant advancements in climate modeling, data resolution, and experimental design.

CMIP6 features higher spatial and temporal resolution in global climate models (GCMs) compared to CMIP5, improving the representation of small-scale processes such as cloud dynamics, land–atmosphere interactions, and extreme events.

CMIP5 used Representative Concentration Pathways (RCPs) to project future emissions, while CMIP6 introduces the Shared Socioeconomic Pathways (SSPs), which provide a more comprehensive socio-economic framework for climate projections.

CMIP6 includes more complex representations of biogeochemical cycles, such as carbon–nitrogen interactions and land-use change impacts, which were either simplified or absent in CMIP5. While CMIP5 and CMIP6 results remain broadly comparable, CMIP6 generally shows stronger climate sensitivities and higher projections of global mean temperature increases, particularly in high-emission scenarios.

3.3. Hydrological Model

Temperature and precipitation data from the high-resolution NASA Earth Exchange Global Daily Downscaled Projections (NEX-GDDP) datasets served as inputs for a hy-

drological model designed to estimate water inflows along the entire Congo River. The hydrological simulations were conducted using the HEC-HMS model, which is designed to represent the full range of hydrological processes and is suitable for both continuous and event-based modeling.

HEC-HMS offers multiple loss methods; however, the Soil Moisture Accounting (SMA) algorithm is particularly effective for long-term watershed soil moisture balance [40]. It is well suited for simulating daily, monthly, and seasonal streamflow.

The SMA algorithm explicitly accounts for all runoff components, including direct runoff (surface flow) and indirect runoff (interflow and groundwater flow) [41–43].

This model requires daily inputs of rainfall, soil conditions, and other hydrometeorological data. In addition to precipitation and temperature, the only other input for the SMA algorithm is the potential evapotranspiration rate.

The potential evapotranspiration was computed using the Oudin formulation [44]. The HEC-HMS model has been used by several researchers and has shown excellent results [42,45,46]. The structure of SMA is described in detail in the HEC-HMS Technical Reference Manual [47].

3.4. Model Calibration

The first phase of this methodology involved calibrating the HEC-HMS model at the Inga outlet. This calibration process utilized 13 CMIP6 and 13 CMIP5 historical datasets, coupled with observed hydrometric data. Consequently, a total of 26 model calibrations were undertaken.

One of the calibration strategies applied encompassed calibrating the model using the entire available dataset, bypassing the conventional validation phase. This strategy capitalizes on extracting maximum information from climate data to shape the parameter set, thereby reducing additional uncertainty linked to selecting calibration and validation periods [48]. Importantly, the statistical enhancement of model performance often arises from expanding the dataset with more years, and the skills required for validation and calibration are not inherently intertwined [49].

Within this study, the HEC-HMS model underwent calibration across the complete available dataset (1981–2000), without following the customary validation step. Due to the model's intricate parameter landscape, a preliminary parameter estimation was derived using insights from the HEC-GeoHMS Extension in tandem with the ArcHydro extension within ArcMap 10.7.1. However, discrepancies in certain physical parameters (such as reach length and slope) emerged from HEC-GeoHMS, necessitating manual rectification through QGIS 3.14.

The primary step in the calibration of the HEC-HMS model involved a manual fine-tuning of model parameters, employing the trial-and-error approach. This methodology empowered the modeler to subjectively adjust parameters, facilitating an appropriate alignment between observed and simulated hydrographs [50]. Subsequently, the Optimization Trials tool integrated within HEC-HMS was employed for automated calibration, serving to refine parameter values.

3.5. Multi-Input Ensemble Modelling

The concept of integrating outputs from different models or methods was explored and applied in the pioneering works of Bates and Dickson [51–54] and others [55,56].

The core idea behind these methods is that each model output captures specific important aspects of the information related to the process being modeled, offering a source of information that may differ from that of other models.

By combining these various sources of information, the user can obtain a comprehensive unified view of the study area [56,57].

Several methods for combining model outputs have been reported, including the simple average method and the weighted average method [56,57], as well as the neural network method [56,58], Bayesian model averaging (BMA) [59], Shuffle Complex Averaging (SCA) [59], and Granger-Ramanathan methods A, B, and C (GRA, GRB, and GRC) [60].

Compared to traditional averaging methods, the GRA method is gaining popularity due to its ability to optimize weights based on performance, making it a superior choice for modeling. In this study, the GRA variant was employed [55] because it is robust, easy to apply, and fast—key criteria for selection in this study.

3.6. Simulations of Hydropower Generation

The planning, design, operations, and financial evaluation of hydropower systems rely on hydrological time series, typically using periods ranging from 20 to 50 years for evaluations [61]. To assess the impact of climate change on hydropower production, production calculations are required, typically conducted using hydropower simulation models. These models capture the key characteristics of the existing hydropower system and are run over multiple years to obtain stable average estimates, both for the current period and for future scenarios. Compared to hydrological models, there are relatively few hydropower simulation models available.

The simplest and most statistical method for calculating power production is by correlating historical records of flow and production [62].

The simplest statistical method for calculating power production is by correlating historical records of flow and production [61].

However, this method is not suitable in all cases. The optimal approach is to use a process-based hydropower simulation, where most of the key components of the hydropower system are defined. In this study, river discharge for the hydropower simulation was modeled using nMA-GRes.xls, an Excel worksheet developed to automate the export of nMAG simulation results into Excel [61].

3.6.1. Hydropower Model Application

Hydropower generation calculations are based on observed daily flows from 1981 to 2000 and simulated daily flows derived from various climate models and emission scenarios. The conversion from flow to power relies on technical data from both existing (Inga 1 and 2) and planned (Inga 3–8) hydropower systems at Inga Falls.

For each generating unit (comprising a turbine and a generator), the power generation is computed as follows:

$$P\ (MW) = 9.81 \times \eta \times Q \times Hn.$$

where:

η is total efficiency in turbine, generator, and transformer.

Q is flow in m^3/s.

Hn is net head (gross head—head loss) in m.

For Inga 1 and 2, efficiency parameters are derived from operational data, whereas Inga 3–8 assumes Francis's turbines with a 96% efficiency, a combined generator + transformer efficiency of 98%, and 1.5% head loss.

The comprehensive (Grand Inga) project is scheduled to unfold in eight phases, with Phase 1 and 2 being existing power plants and Phase 3 to 8 being in the planning stages. The various phases encompass different numbers of units, utilizing the full 150 m head, except for Phase 1 and 2, which utilize only a limited part of it. The augmentation of head is accomplished by constructing a substantial dam across the river, elevating the intake

level to 150 m. A minimum bypass flow of 10% of average flow (3700 m^3/s) is stipulated for all simulations.

The division of the project into multiple stages is primarily designed to illustrate the points at which climate change impacts become significant in the development process. This approach allows for a clear assessment of how different stages of the project may be influenced by climate variability and change.

A key reason for this staged approach is to demonstrate that the early phases of development at Inga Falls can proceed with minimal climate risk. The hydrological stability of the Congo River ensures that the initial stages of the project remain largely unaffected by climate change. However, as the development progresses and expands, the potential influence of climate change on water availability and operational efficiency becomes more relevant.

3.6.2. Steps of the Hydropower Generation Simulation Project

1. Define the hydropower model for existing and prospective developments in Inga Falls.
2. Generate power from observed flow from 1981 to 2000 (Baseline, 1 Run).
3. Generate power from flow data acquired from 13 Climate models for 1981–2000 (13 runs).
4. Produce generation from future flow data under two main climate modeling scenarios: CMIP5 and CMIP6, each involving different models, RCP/SSP scenarios, and time frames, leading to 65 different runs per scenario.
5. Compile summary results for all models and emission scenarios.

4. Results and Discussion

This section presents the findings on hydrological modeling, climate scenario forecasts, future hydrological simulations, and projected energy production.

4.1. Hydrological Modelling

As started in the methodological section, the HEC-HMS model has been calibrated based on the data available at the Inga outlet. The historical datasets of 13 NEX-GDDP-CMIP6 and their CMIP5 predecessors for the 1981–2000 period have been used for the model development. The GRC weighting approach was used to determine weights based on the comparison between simulated and observed hydrographs. These weights were then applied to the 13 model members to generate a single weighted hydrograph, which was evaluated using the Nash–Sutcliffe Efficiency metric for both CMIP6 and CMIP5. The calibrated weights for each hydrograph were subsequently used for model simulations under future climate scenarios. For brevity, detailed calibration results are not included. Hydrological modeling utilized daily precipitation and temperature data, while model calibration was conducted using daily streamflow data. Figure 3 summarizes the simulation of daily streamflow patterns during the calibration period.

4.2. Projected Hydrologic Scenario

Following the analysis of projected climate variables, the corresponding hydrological scenarios were evaluated. Basin streamflow was simulated by inputting the projected climate data into the previously calibrated hydrological model. Future runoff generation results from the combined influence of precipitation and temperature projections. Figure 4 illustrates the future streamflow patterns for each model scenario, comparing them with historical flow data.

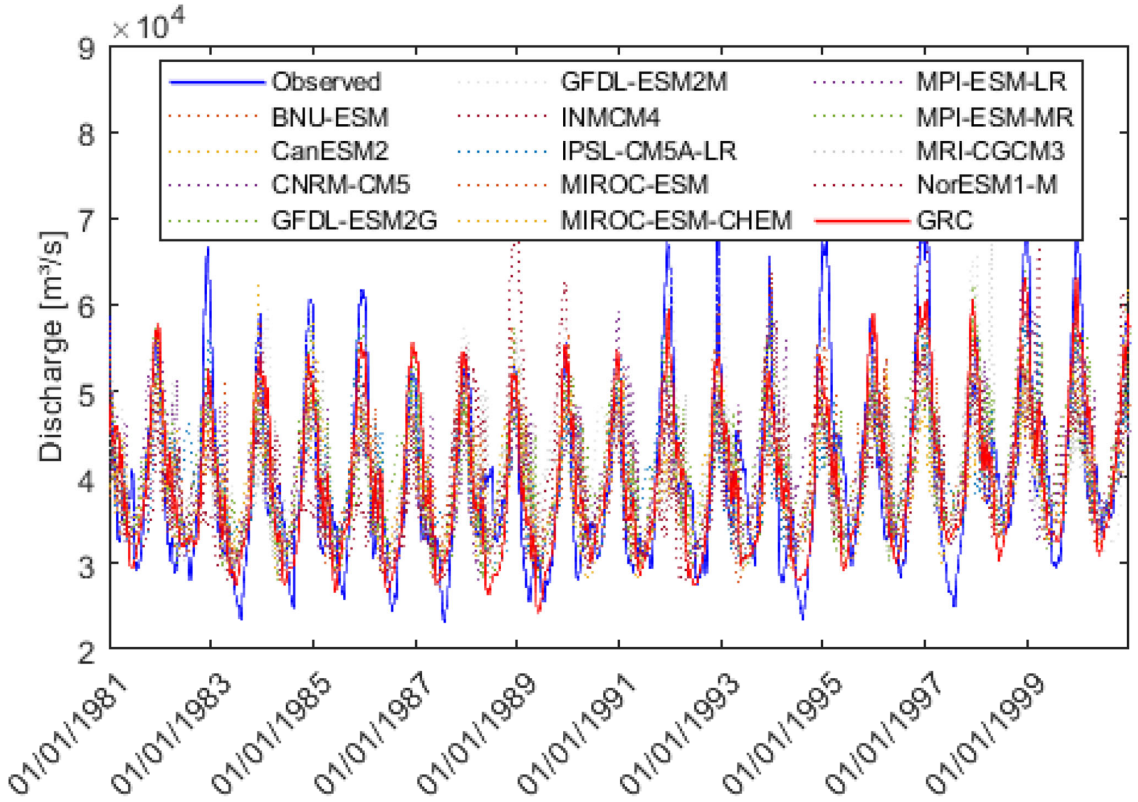

Figure 3. HEC-HMS model calibration for years 1981–2000; dashed lines indicate hydrographs of 13 CMIP5 members and solid line indicates observed flows (blue) and GRC average (red).

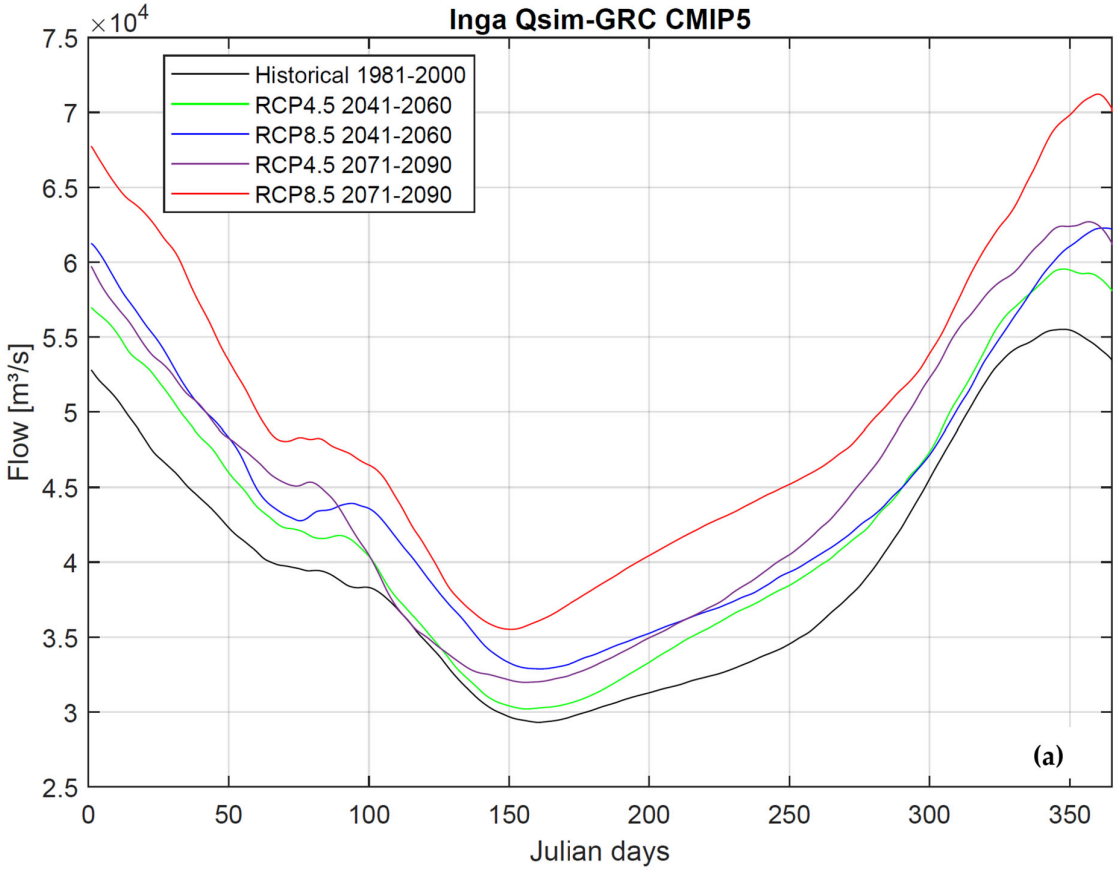

Figure 4. *Cont.*

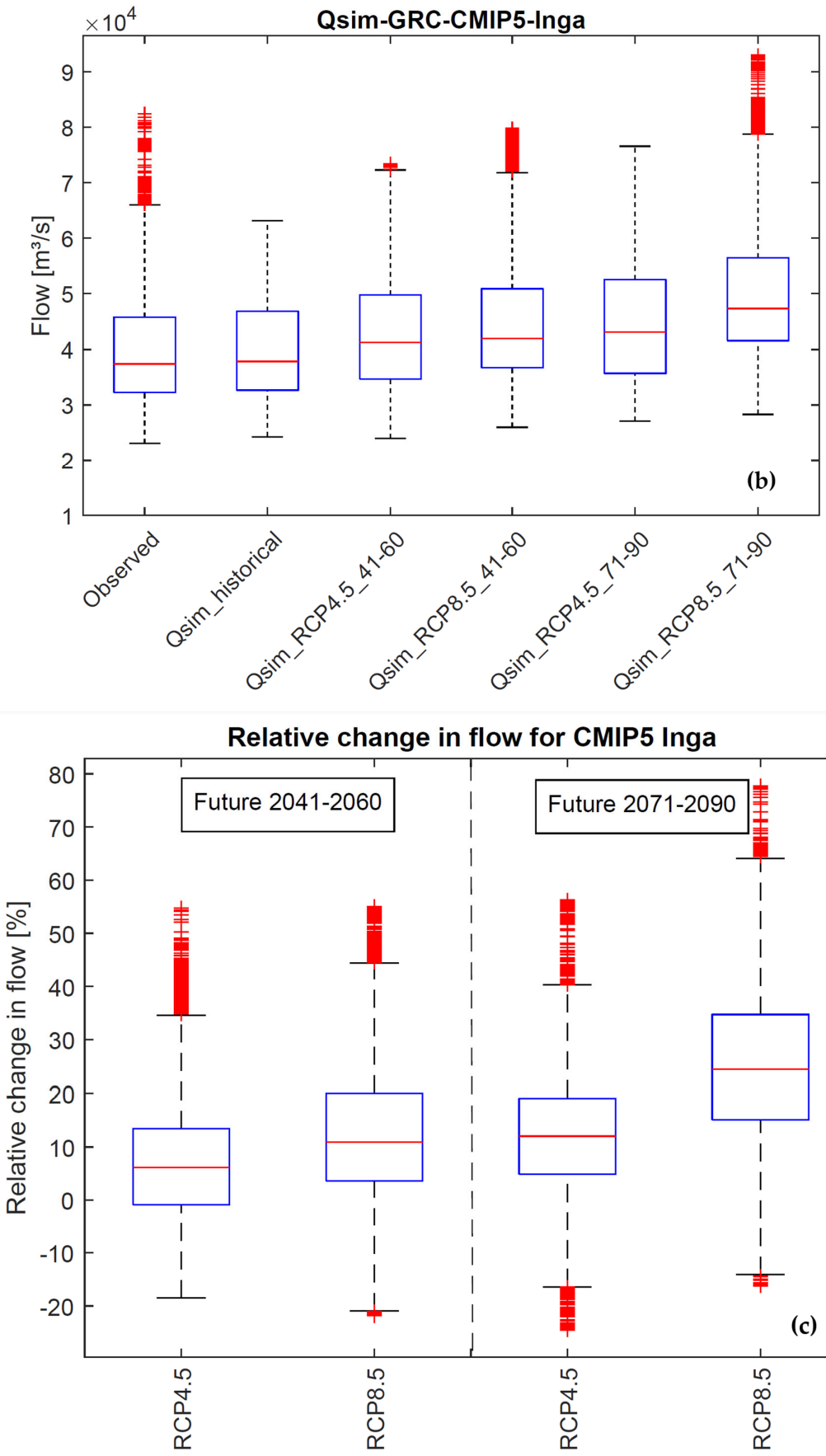

Figure 4. The annual GRC average flow of the Congo River at the Inga Falls gauging station is shown for the reference period (1981–2000) and projected future periods under different emission scenarios in panels (**a**,**b**). Panel (**c**) illustrates the relative change in percentage.

4.3. Hydropower Generation Simulations

4.3.1. Flow Duration Curve

The flow duration curve (FDC) was generated using the GRC daily discharge simulated from the HEC-HMS model, averaged over 20 years for both the baseline period and future time periods under CMIP5 and CMIP6 scenarios (Figures 5 and 6).

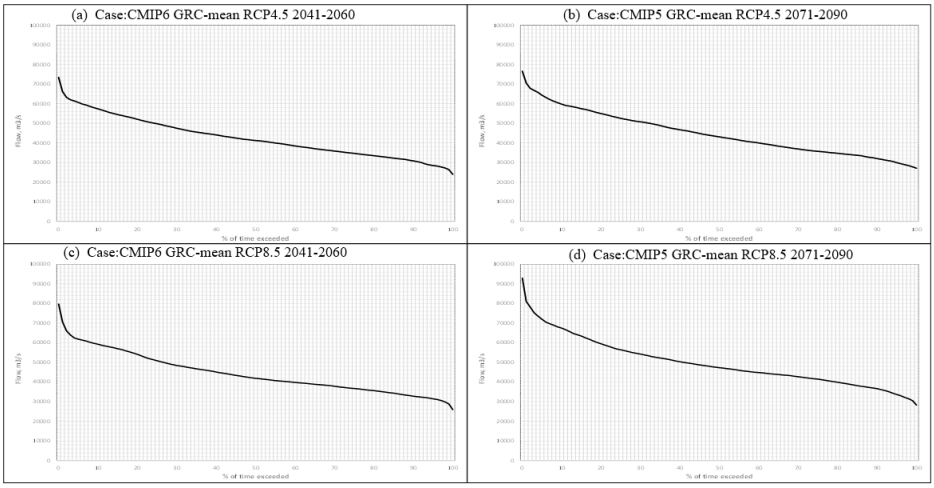

Figure 5. Flow duration curve of Inga Falls for GRC CMIP5 scenarios.

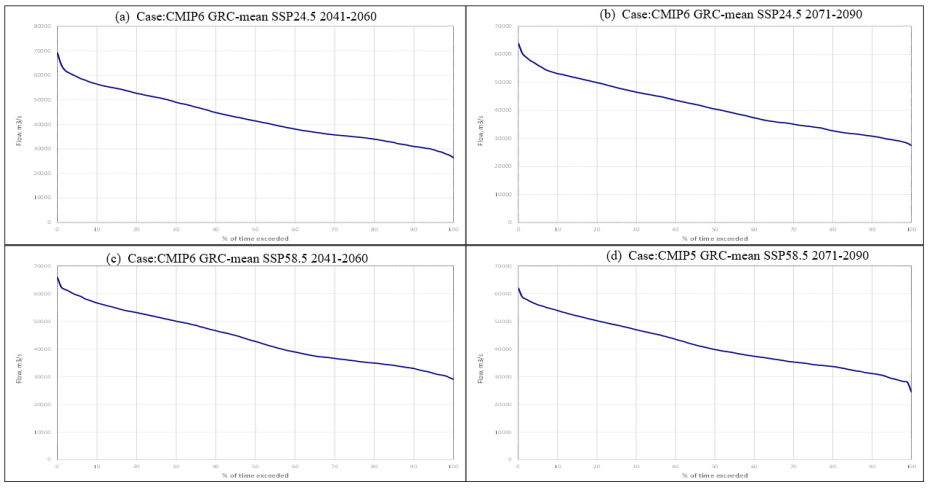

Figure 6. Flow duration curve of Inga Falls for GRC CMIP6 scenarios.

This FDC presents, for Inga Falls, the duration during which a certain flow value is reached or exceeded for both CMIP5 and CMIP6 scenarios. It allows the selection of the nominal flow rate of the projected installation by considering the reserved flow rate and the technical minimum flow rate of the equipment. It also makes it possible to estimate the power of the plant and its average annual production.

Its distribution throughout the year is necessary for economic reasons since the sales prices applied to independent producers vary with the seasons of the year and the hours of the day.

4.3.2. Water Utilization Duration Curve

The minimum bypass (environmental) flow of 3700 m^3/s requires water. At full development, up to and including Inga 8, the maximum flow that can be utilized in power plants is 36,800 m^3/s + 3700 m^3/s, or 40,500 m^3/s. Any flow larger than this will lead to flood spill at the dam. The maximum power capacity at this flow (36,800 m^3/s)

is 47,544 MW. This is equivalent to 1.14 TWh/day. Figures 7 and 8 show total water utilization for Inga Falls for CMIP5 and CMIP6, respectively, based on simulated flow for all scenarios. It is observed that there is ample water to maintain full capacity in the turbines approximately 40% of the time, while Inga 6, 7, and 8 will experience intervals where full generation capacity is not attainable.

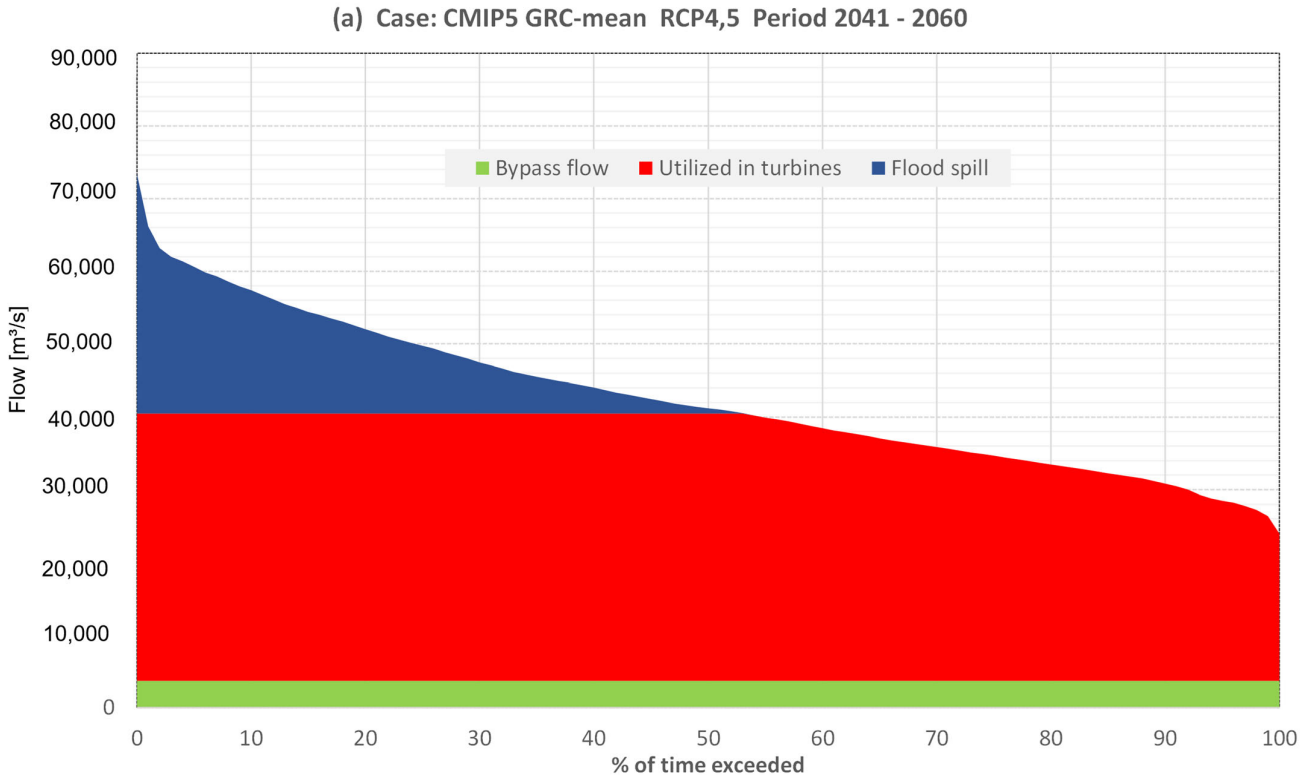

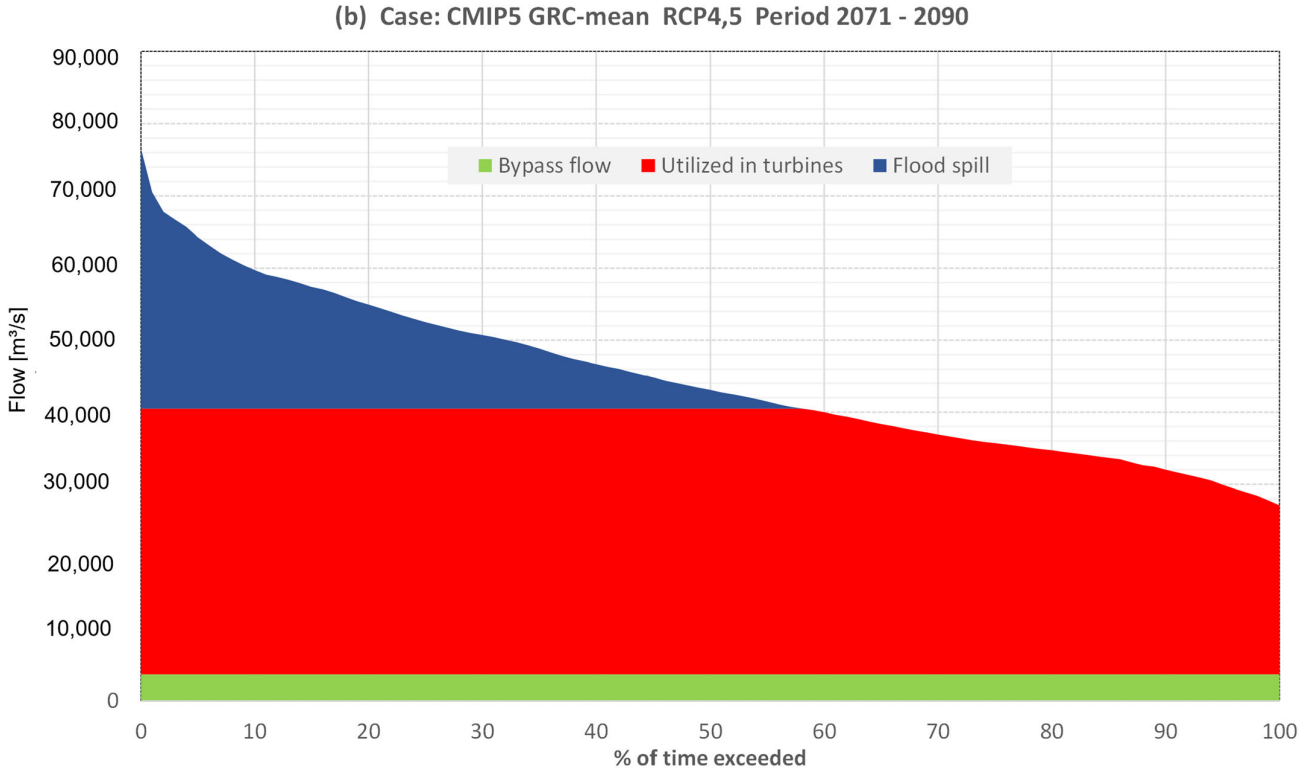

Figure 7. *Cont.*

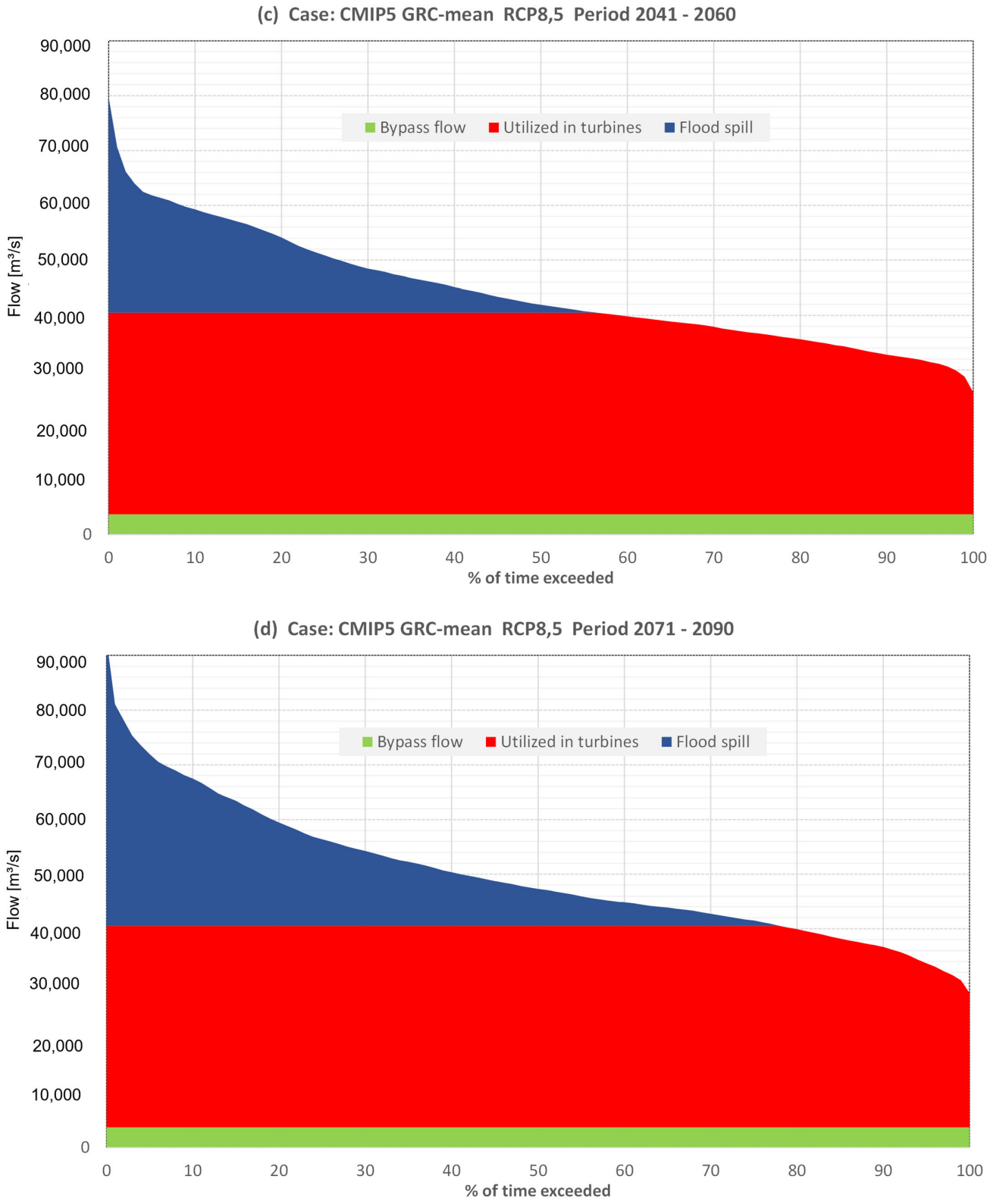

Figure 7. Water utilization duration curve of Inga Falls for GRC CMIP5 scenarios.

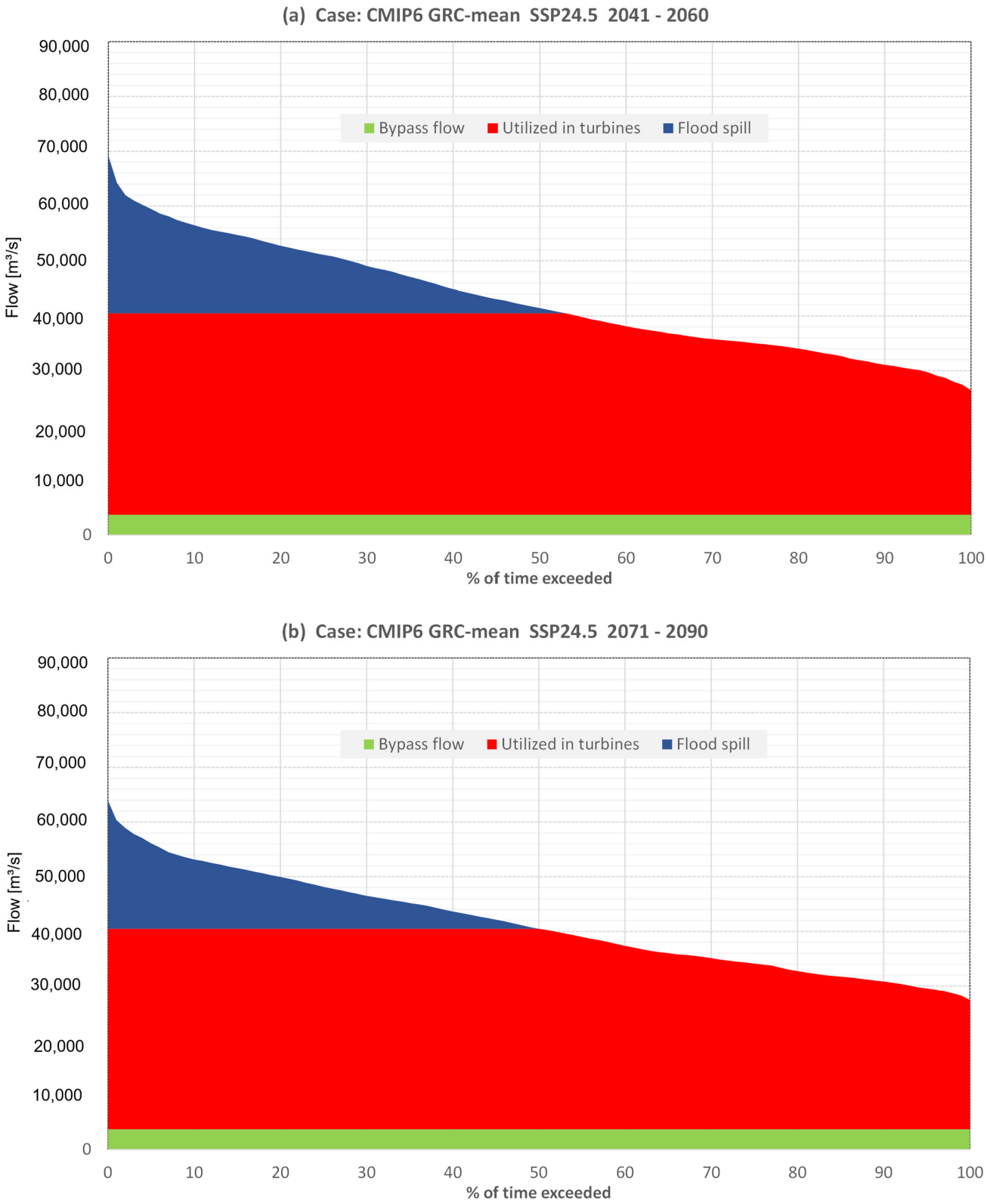

Figure 8. *Cont.*

Figure 8. Water utilization duration curve of Inga Falls for GRC CMIP6 scenarios.

Power generation is simulated daily, prioritizing water use as follows:

1. Minimum flow (3700 m^3/s)—Highest Priority.
2. Units in Phase 1—Second Priority.
3. Units in Phase 2—Third Priority.
4. Units in Phases 3 to 8—Decreasing Order of Priority.

4.3.3. Hydropower Generation from Observed Flow 1981–2000

Historically (1981–2000), the minimum flow at Inga Falls has been 23,063 m^3/s. The total capacity for Phase 1 and Phase 2 power plants is only 3580 m^3/s ($6 \times 130 + 8 \times 252.5$), and therefore, there will always be enough water to run Inga 1 and 2 at full capacity and still supply the minimum flow of 3700 m^3/s. In fact, there will nearly always be water enough to also meet the full capacity for Inga 3, Inga 4, and Inga 5. But with the introduction of Inga 6, there will be episodes where the available flow is not always enough to run at full capacity, and the number of such episodes will increase for each phase. This is illustrated by Figure 9.

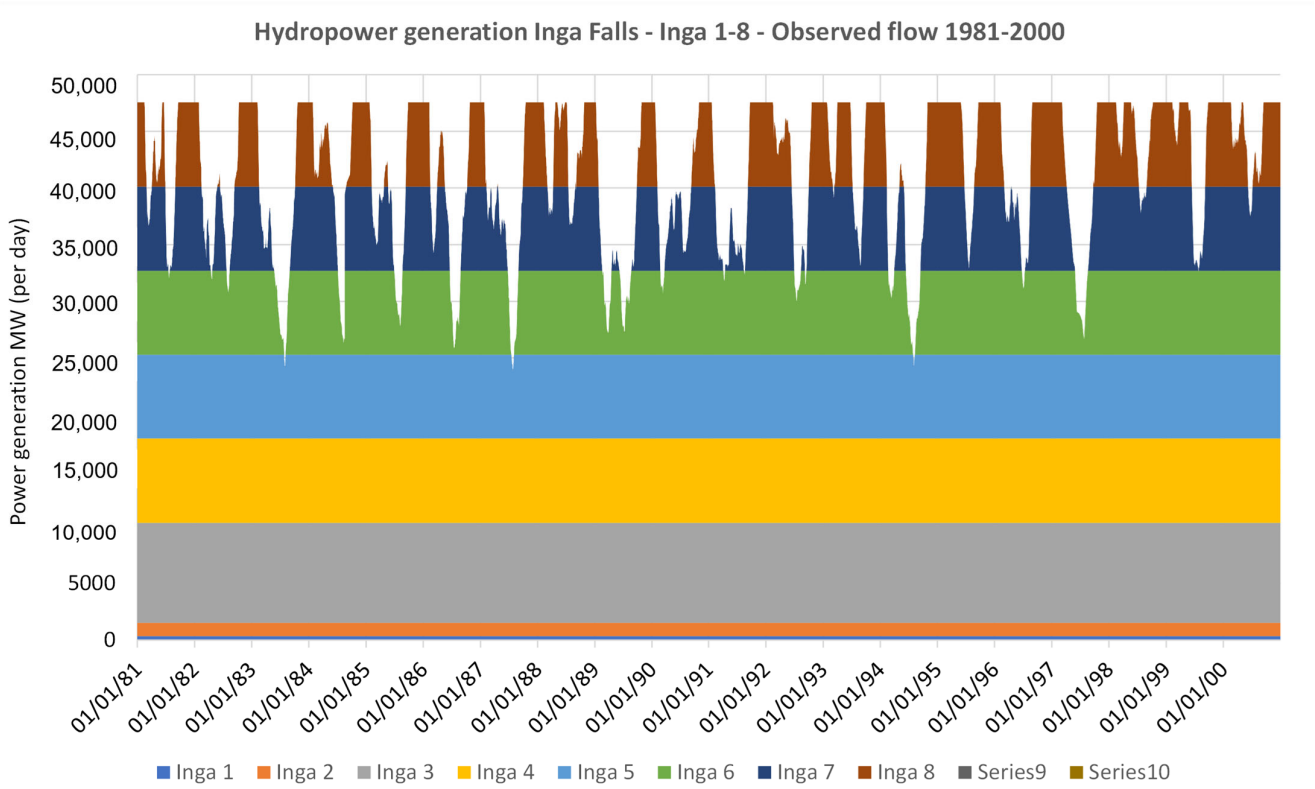

Figure 9. Hydropower generation for Inga 1 to Inga 8 based on data from the years 1981–2000.

Figure 9 shows simulated generation (MW) each day during the historic period of 1981–2000. The results are stacked to make it easy to see if there is a reduced generation due to limiting flow. We can see that power plants in Phase 1 to 5 almost always generate at full capacity, while those in Phase 6, 7, and 8 have increasing episodes of reduced or no generation due to shortage of water (Phase 5 has a few days with flow slightly below capacity). The average number of Full Load Hours (FLH) and Capacity Factor (Cf) was computed for each simulation, and the results are shown in Table 4, in the two rightmost columns. The duration curves for Inga 6, 7, and 8 are shown in Figure 10. Increasing the installed capacity beyond Inga 8 is probably not economically viable, but we have still computed and presented the results in Table 4.

Table 4 shows that the Full Load Hours (FLH) and Capacity Factor (Cf) decline from 8760 h and 100% for Inga 1 to Inga 5 down to 4221 h and 48% for Inga 8.

Main generation results for each phase are shown in Table 4. The results are computed cumulatively, as flow (Q_{max}), power (P_{max}), and average annual energy generation (Energy) for each phase from Inga 1 up to and including this phase. Computed energy generation of a fully developed system (Inga 1 to Inga 8) would give an average annual generation of 360 TWh/year, practically 1 TWh/day.

Table 4. Inga Falls—Main results for simulated hydropower generation (1981–2000).

	Cumulative Values		Results for 1981–2000		
	Q_{max}	P_{max}	Energy	FLH	C_f
Phase	**m^3/s**	**MW**	**TWh/yr**	**hours**	**%**
Inga 1	780	351	2.4	8760	100
Inga 2	2800	1495	10.4	8760	100
Inga 3	9400	10,434	88.7	8760	100
Inga 4	14,880	17,856	153.7	8760	100
Inga 5	20,360	25,278	218.7	8756	100
Inga 6	25,840	32,700	280.5	8320	95
Inga 7	31,320	40,122	328.8	6510	74
Inga 8	36,800	47,544	360.1	4221	48

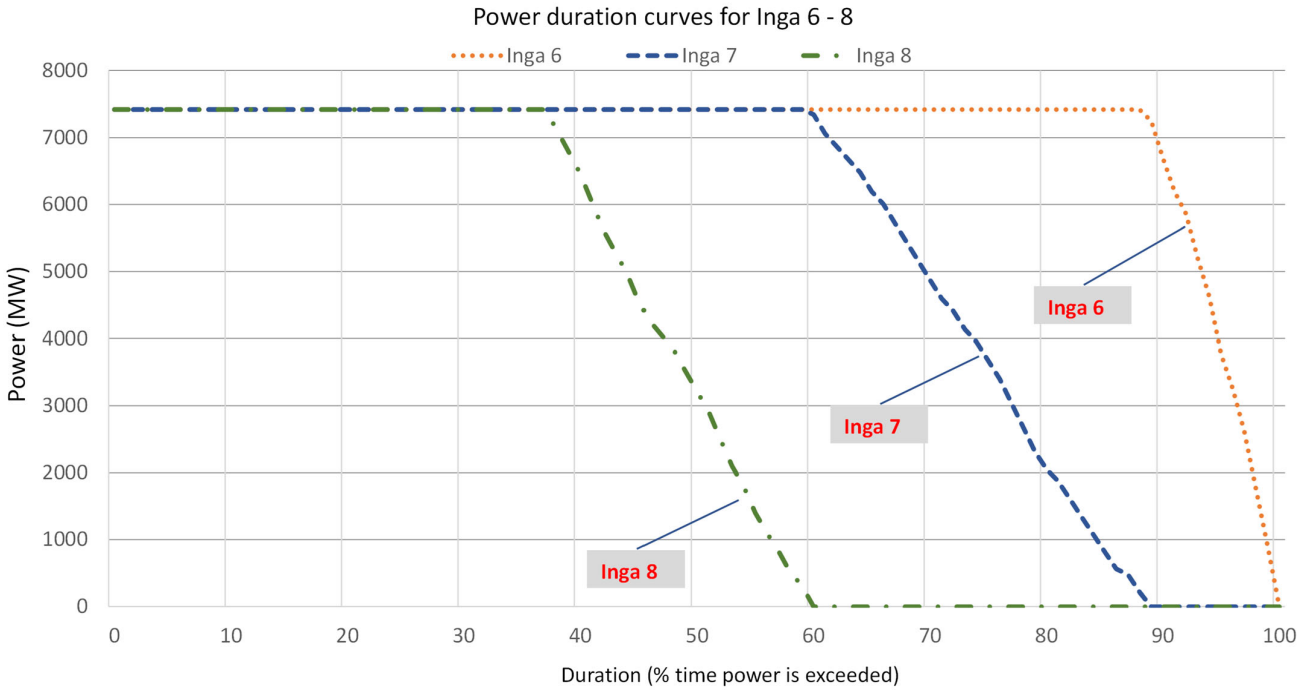

Figure 10. Power duration curves for Inga 6, 7, and 8. Historical period: 1981–2000.

4.3.4. Hydropower Generation from Each Future Simulation

Each of the future simulations (model run) is performed with a timeseries of 20 years (like 1981–2000) flow data, and the hydropower system as described above. This results in a time series of hydropower generation (MW/day) for each of the eight phases. The results are summarized into the following main statistics:

Average annual generation Inga 1–2

Average annual generation Inga 3–8

For this study, the generation in existing power plants Inga 1 and 2 is not affected by climate change and is therefore not used further. There will always be enough water for full supply even after possible climate change. The key results on changes in hydropower generation due to climate change for CMIP5 and CMIP6 are summarized in Tables 5–7. Figure 11 illustrates the simulated variations in hydropower generation across all future scenarios for both CMIP5 and CMIP6.

Table 5. Main Results of CMIP5.

	IPCC Asessment	Emission Scenario	Time period	Simulated hydropower generation (TWh/year) for power plant units included in Inga Phase 3 to Phase 8													Average	Average	Average
				BNU-ESM	**CanESM2**	**CNRM-CM5**	**GFDL-ESM2G**	**GFDL-ESM2M**	**inmcm4**	**IPSL-CM5A-LR**	**MIROC-ESM**	**MIROC-ESM-CHEM**	**MPI-ESM-LR**	**MPI-ESM-MR**	**MRI-CGCM3**	**NorESM1-M**	**Average All 13 Models**	**Ensamble Average All 13 Models**	**GRC-Average**
Simulated annual generation, CMIP5	CMIP5	-	1981–2000	363.8	370.8	367.7	365.2	367.9	358.7	368.0	366.8	361.9	369.7	371.6	372.3	365.9	366.9	371.5	355.0
	CMIP5	RCP4.5	2041–2060	352.6	364.3	374.3	372.7	372.2	362.9	389.7	346.1	336.5	385.9	385.2	376.3	375.3	368.8	377.2	367.8
	CMIP5	RCP4.5	2071–2090	361.2	363.7	379.6	372.9	366.4	360.9	395.8	336.0	335.9	384.2	387.7	379.2	380.6	369.5	378.9	374.6
	CMIP5	RCP8.5	2041–2060	357.1	368.5	372.2	368.8	380.5	373.4	397.8	343.9	330.4	386.1	386.0	381.7	376.8	371.0	381.6	378.5
	CMIP5	RCP8.5	2071–2090	366.8	365.2	380.2	378.0	380.9	374.4	400.9	353.9	355.1	396.0	395.6	381.0	396.0	378.8	390.8	392.7

Table 6. Main Results of CMIP6.

	IPCC Asessment	Emission Scenario	Time period	Simulated hydropower generation (TWh/year) for power plant units included in Inga Phase 3 to Phase 8													Average	Average	Average
				BNU-ESM	**CanESM2**	**CNRM-CM5**	**GFDL-ESM2G**	**GFDL-ESM2M**	**inmcm4**	**IPSL-CM5A-LR**	**MIROC-ESM**	**MIROC-ESM-CHEM**	**MPI-ESM-LR**	**MPI-ESM-MR**	**MRI-CGCM3**	**NorESM1-M**	**Average all 13 models**	**Ensamble Average all 13 models**	**GRC-Average**
Simulated annual generation, CMIP6	CMIP6	-	1981–2000	369.8	374.7	379.6	378.9	378.7	369.3	369.9	374.2	373.0	376.0	376.5	379.5	371.4	374.7	377.5	363.8
	CMIP6	SSP24.5	2041–2060	358.6	379.5	376.5	361.0	365.2	398.9	380.2	377.1	380.2	383.6	385.4	378.9	376.1	377.0	380.2	369.1
	CMIP6	SSP24.5	2071–2090	355.8	379.5	370.6	359.5	358.4	399.7	397.9	373.4	384.9	373.4	385.2	378.9	381.7	376.8	381.2	365.5
	CMIP6	SSP58.5	2041–2060	353.2	382.5	383.9	366.5	350.4	402.0	388.5	374.2	380.2	388.7	394.6	378.0	383.7	378.9	384.5	375.3
	CMIP6	SSP58.5	2071–2090	345.0	373.5	365.7	352.8	331.9	403.6	402.0	370.2	383.9	398.0	399.7	365.3	379.5	374.7	387.2	366.4

Table 7. Key Findings on Hydropower Generation Changes Due to Climate Change.

	IPCC Asessment	Emission Scenario	Time period	**BNU-ESM**	**CanESM2**	**CNRM-CM5**	**GFDL-ESM2G**	**GFDL-ESM2M**	**inmcm4**	**IPSL-CM5A-LR**	**MIROC-ESM**	**MIROC-ESM-CHEM**	**MPI-ESM-LR**	**MPI-ESM-MR**	**MRI-CGCM3**	**NorESM1-M**	**Average all 13 models**	**Ensamble Average all 13 models**	**GRC-Average**
Relative change - CMIP5	CMIP5	RCP4.5	2041–2060	0.97	0.98	1.02	1.02	1.01	1.01	1.06	0.94	0.93	1.04	1.04	1.01	1.03	1.00	1.02	1.04
	CMIP5	RCP4.5	2071–2090	0.99	0.98	1.03	1.02	1.00	1.01	1.08	0.92	0.93	1.04	1.04	1.02	1.04	1.01	1.02	1.05
	CMIP5	RCP8.5	2041–2060	0.98	0.99	1.01	1.01	1.03	1.04	1.08	0.94	0.91	1.04	1.04	1.03	1.03	1.01	1.03	1.07
	CMIP5	RCP8.5	2071–2090	1.01	0.98	1.03	1.03	1.04	1.04	1.09	0.96	0.98	1.07	1.06	1.02	1.08	1.03	1.05	1.11
Relative change - CMIP6	CMIP6	SSP24.5	2041–2060	0.97	1.01	0.99	0.95	0.96	1.08	1.03	1.01	1.02	1.02	1.02	1.00	1.01	1.01	1.01	1.01
	CMIP6	SSP24.5	2071–2090	0.96	1.01	0.98	0.95	0.95	1.08	1.08	1.00	1.03	0.99	1.02	1.00	1.03	1.01	1.01	1.00
	CMIP6	SSP58.5	2041–2060	0.96	1.02	1.01	0.97	0.93	1.09	1.05	1.00	1.02	1.03	1.05	1.00	1.03	1.01	1.02	1.03
	CMIP6	SSP58.5	2071–2090	0.93	1.00	0.96	0.93	0.88	1.09	1.09	0.99	1.03	1.06	1.06	0.96	1.02	1.00	1.03	1.01

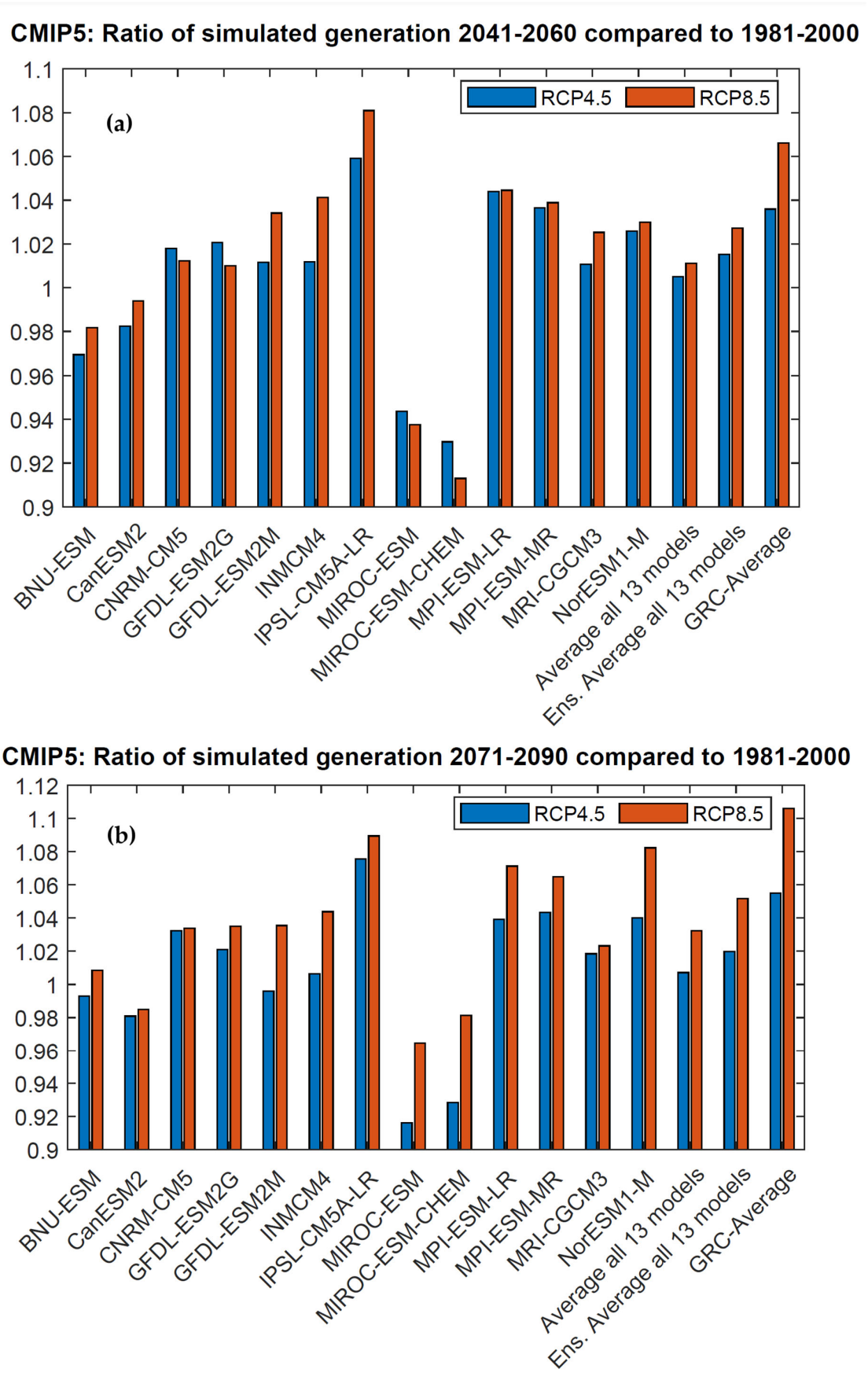

Figure 11. *Cont.*

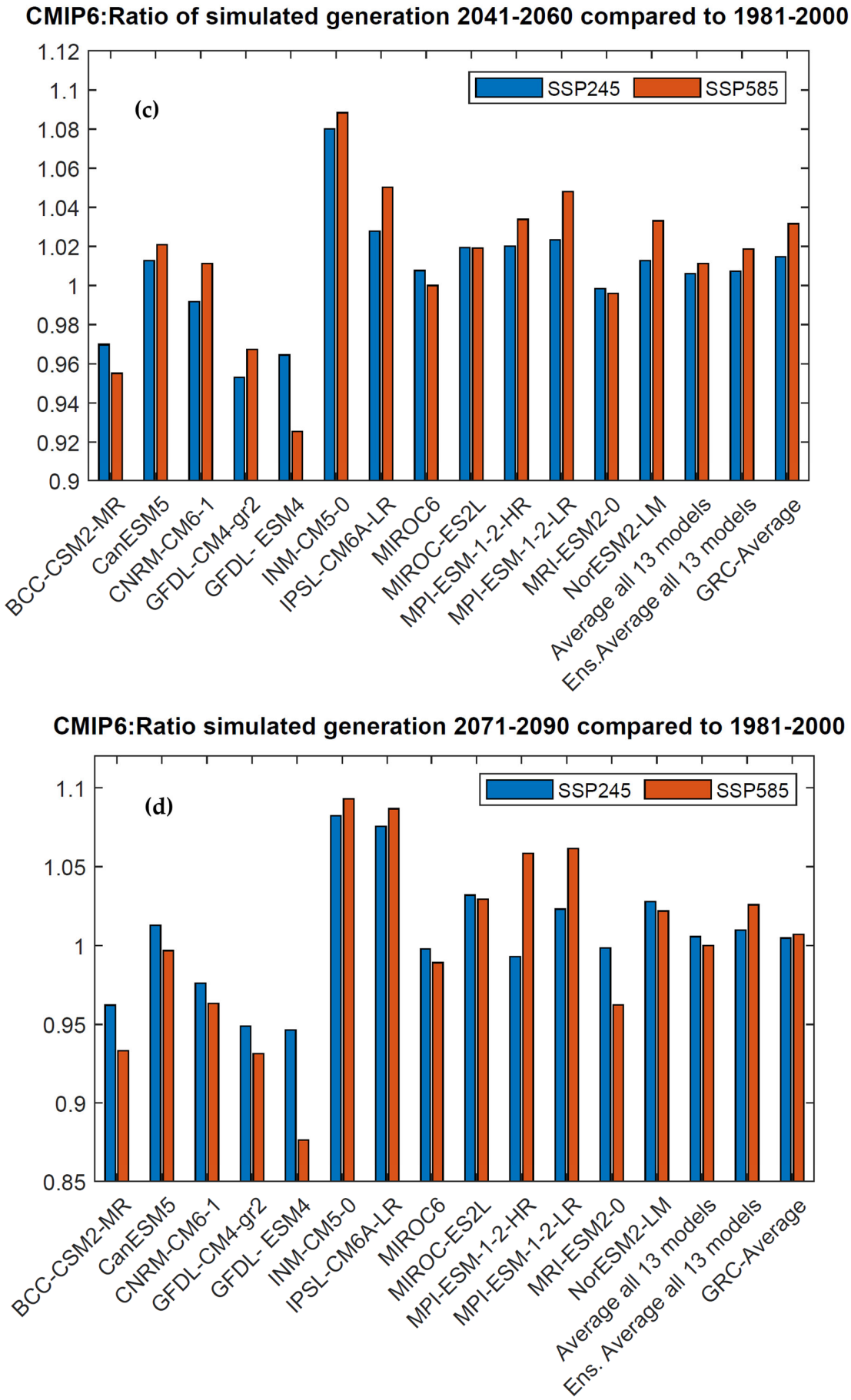

Figure 11. Simulated change in hydropower generation for CMIP5 (**a**,**b**) and CMIP6 (**c**,**d**).

Table 7 shows the ratio between simulated annual generation in Inga 3–8 and simulated generation during 1981–2000 for the same model.

Hydropower Generation from CMIP5 Scenarios

Table 7 presents the projected changes in the ensemble mean and range of hydropower potential relative to the reference period under different RCP scenarios. The mean annual power (MAP) generally shows an increase across both future time horizons.

As for the historical period (1981–2000) (Figure 9), in all CMIP5 futures scenarios there will always be enough water to operate Inga 1, Inga 2, Inga 3, Inga 4, and Inga 5 at their maximum capacity while ensuring a minimum flow rate of 3700 m^3/s. This historical stability underscores the reliability of the system during that time frame.

However, unlike the historical period, the number of episodes introduced from Inga 6 decreases significantly in the RCP4.5 scenario and almost disappears in the RCP8.5 scenario.

This positive change is a consequence of the increase of river flow patterns anticipated in the future.

As we move further along to the Inga 7 and Inga 8 phases, the episodes of favorable conditions persist, but they exhibit a less pronounced presence compared to the historical period. This phenomenon can be attributed to the projected increase in river flow for these future periods, which necessitates a more nuanced assessment of water availability and utilization.

To visually encapsulate these findings, please refer to Figure 12, which graphically illustrates the evolving dynamics of water supply and its impact on the various Inga phases.

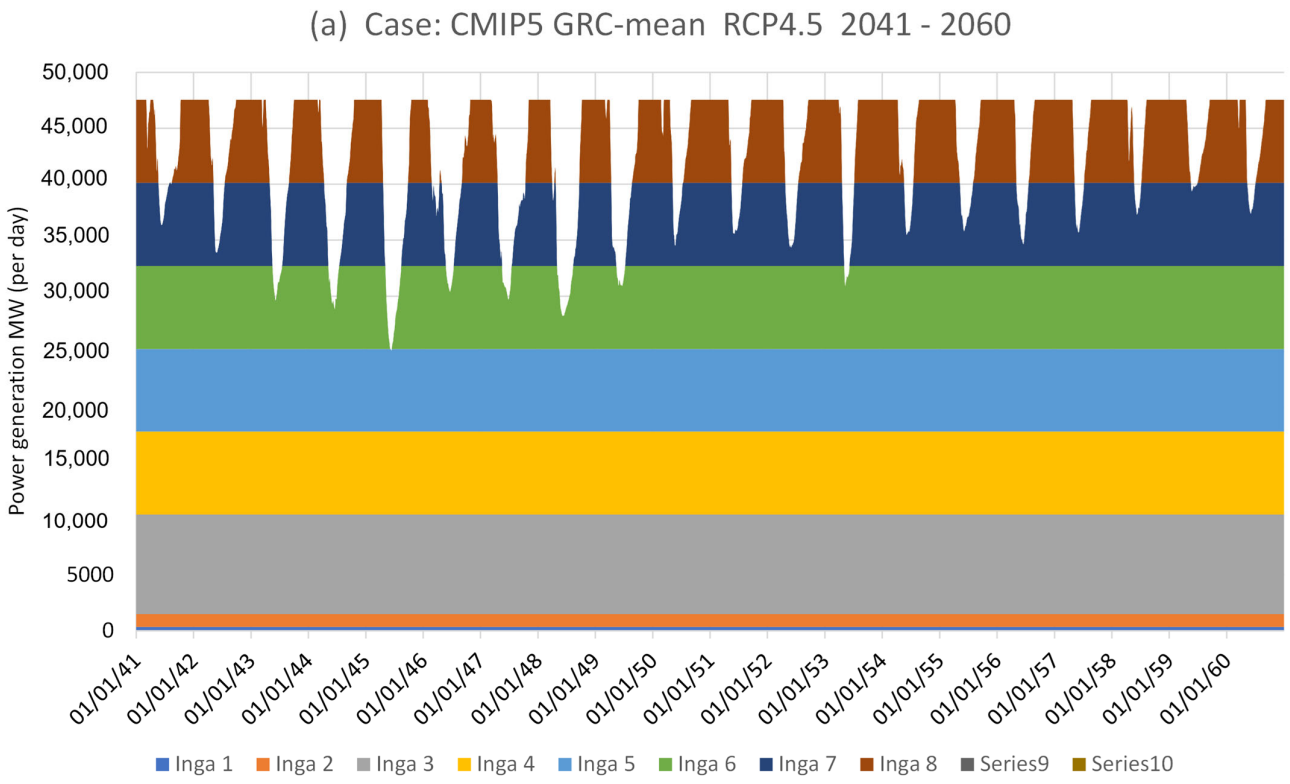

Figure 12. *Cont.*

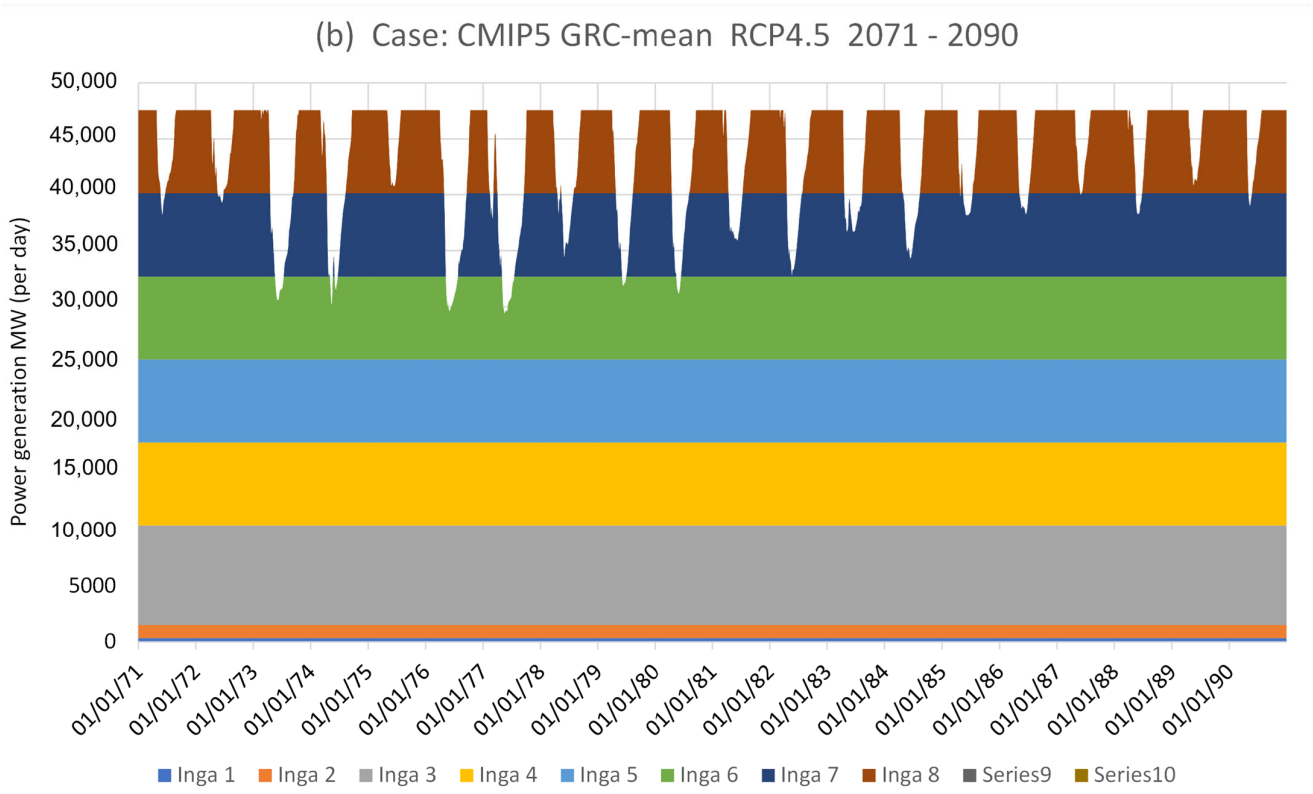

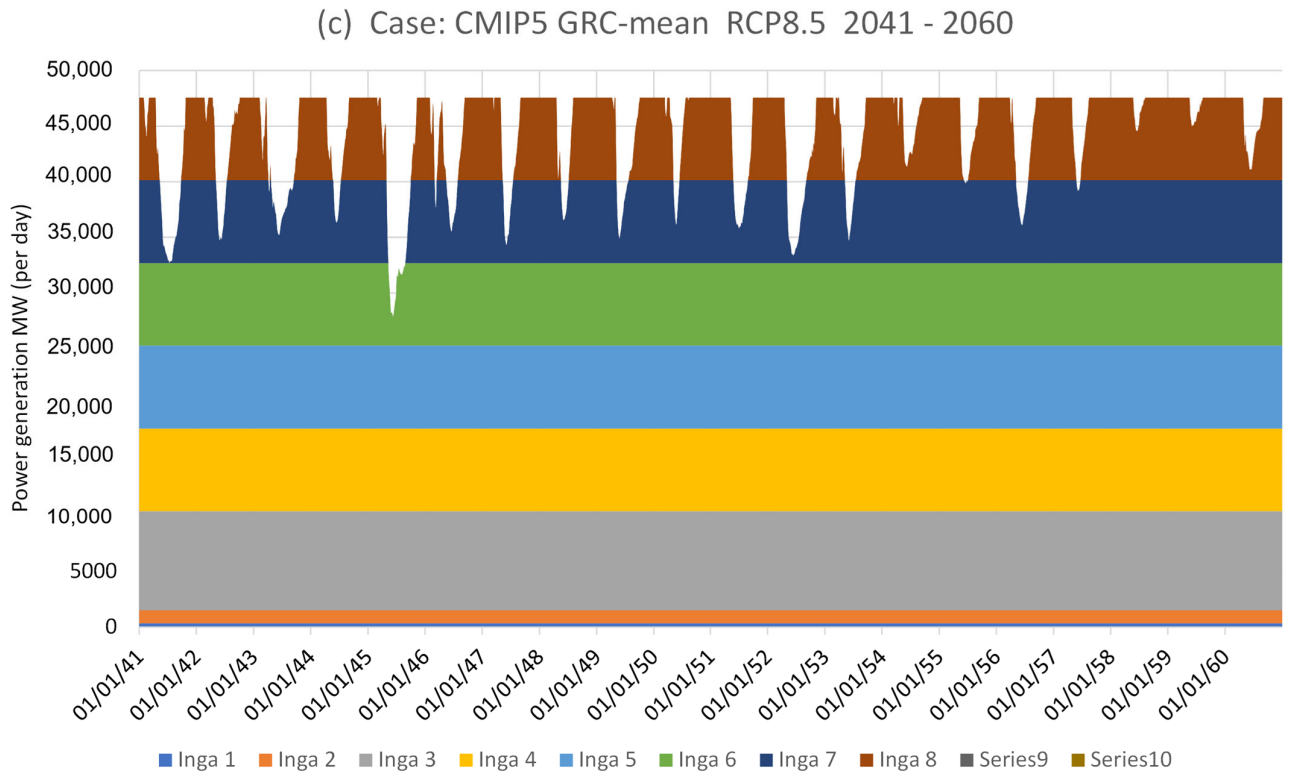

Figure 12. *Cont.*

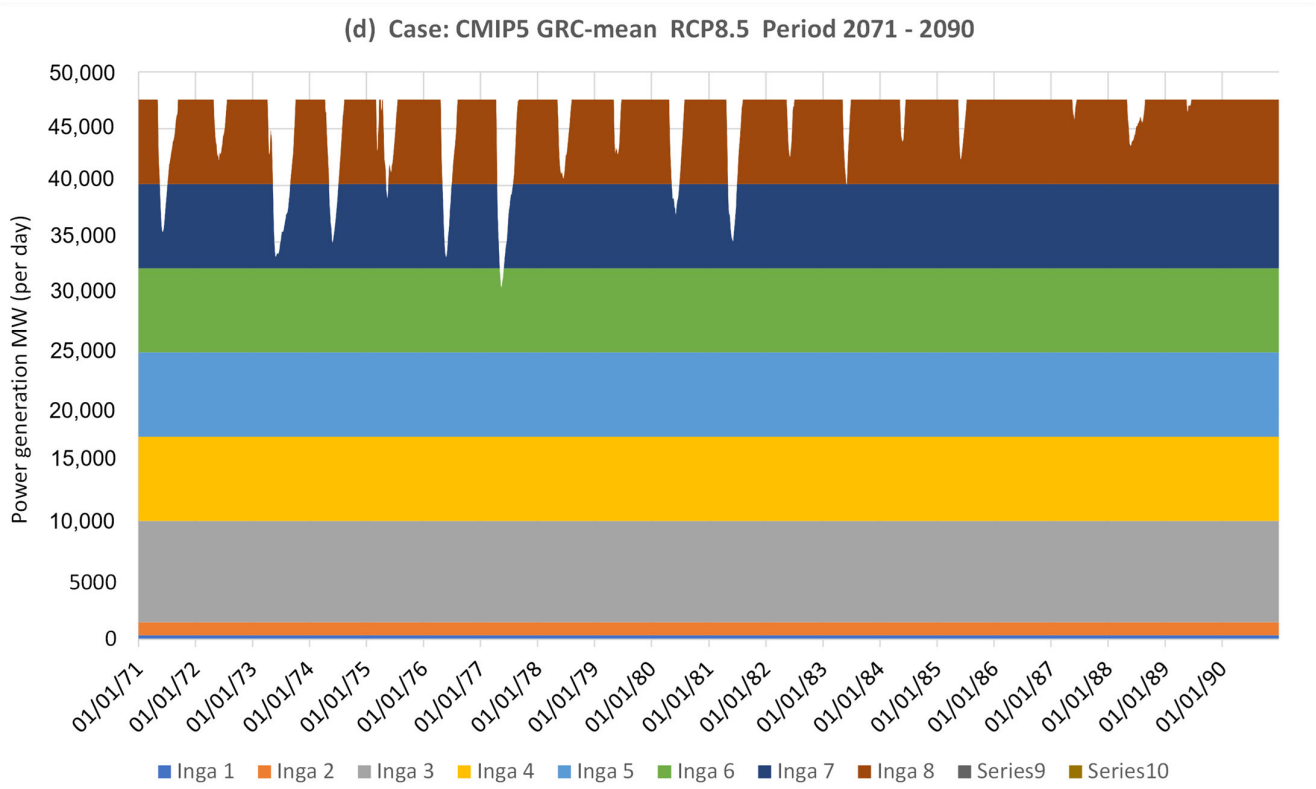

Figure 12. Hydropower generation at Inga Falls for GRC CMIP5 scenarios.

Hydropower Generation from CMIP6 Scenarios

Hydroelectric production under the CMIP6 scenarios closely mirrors that of the CMIP5 scenarios. This consistency in outcomes is vividly depicted in Figure 13, where it becomes evident that all CMIP6 scenarios exhibit a strikingly similar pattern to that observed in CMIP5.

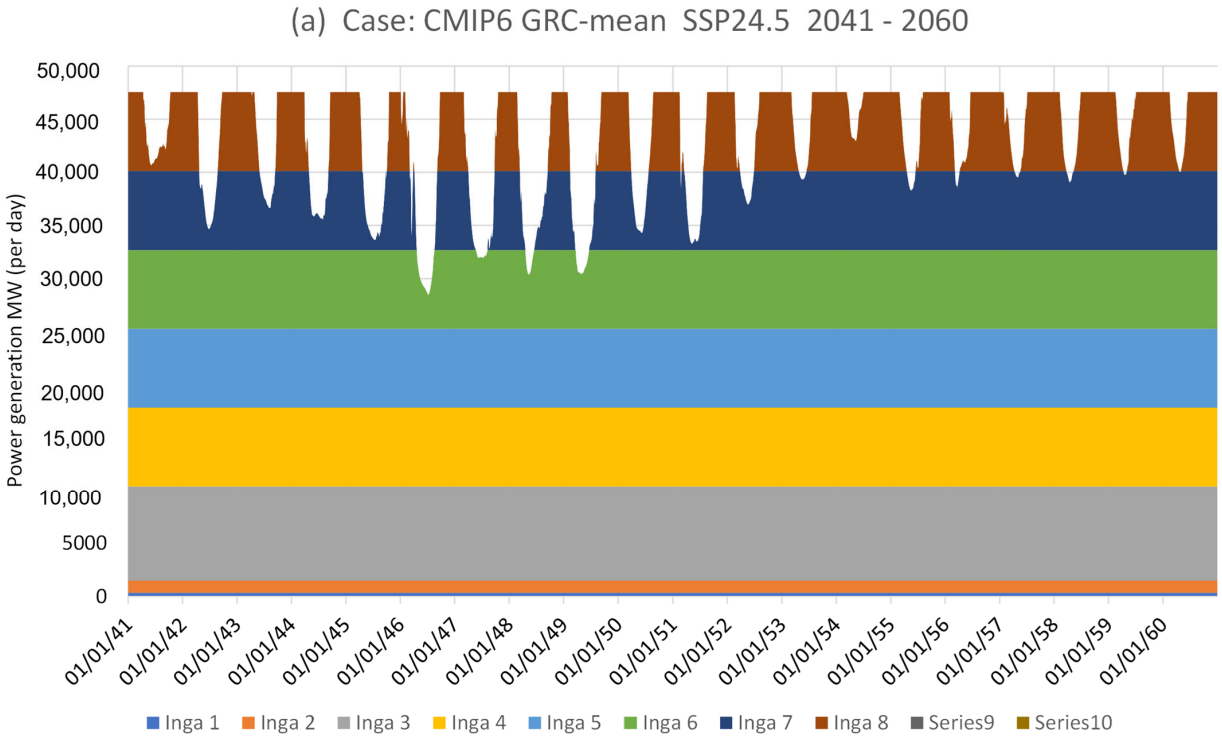

Figure 13. *Cont.*

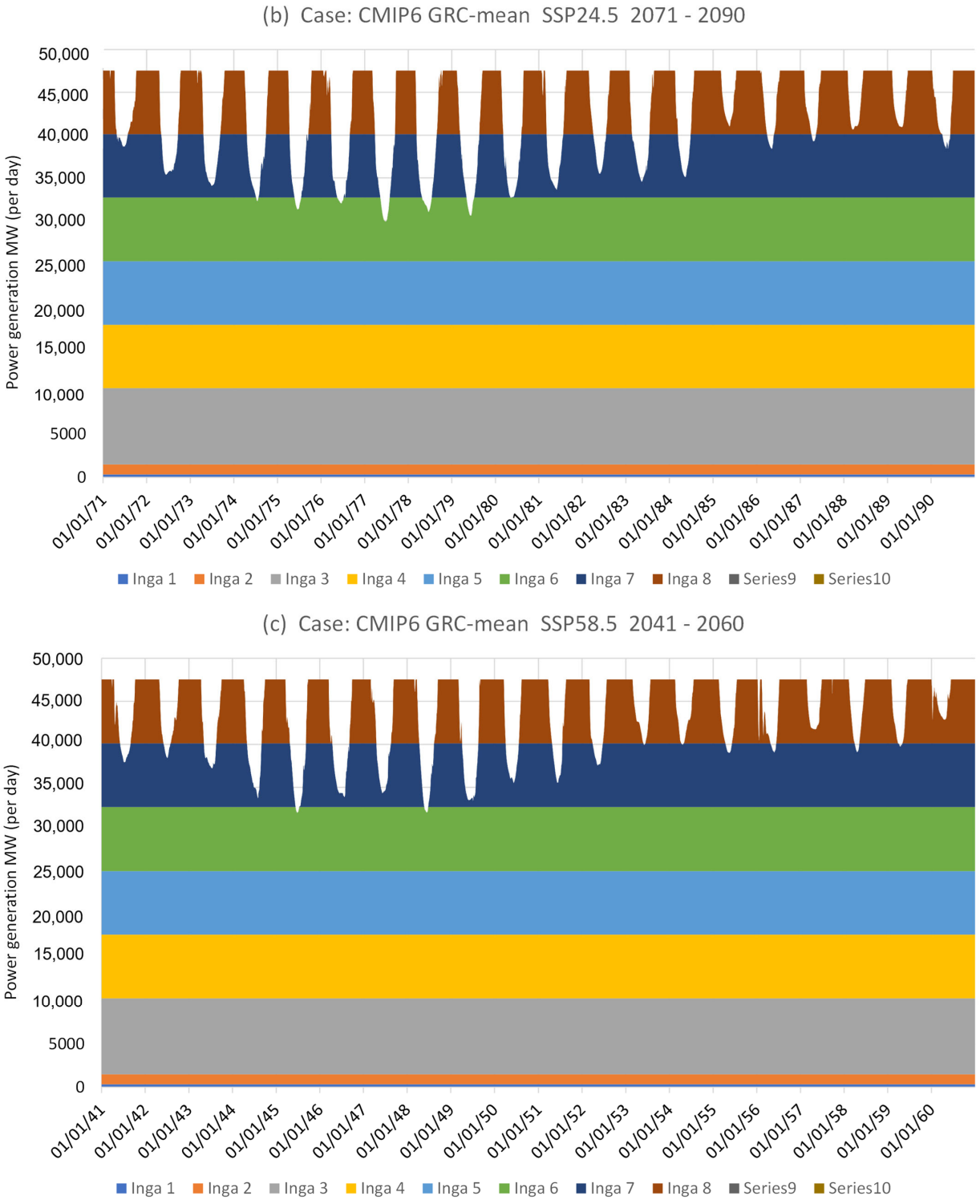

Figure 13. *Cont.*

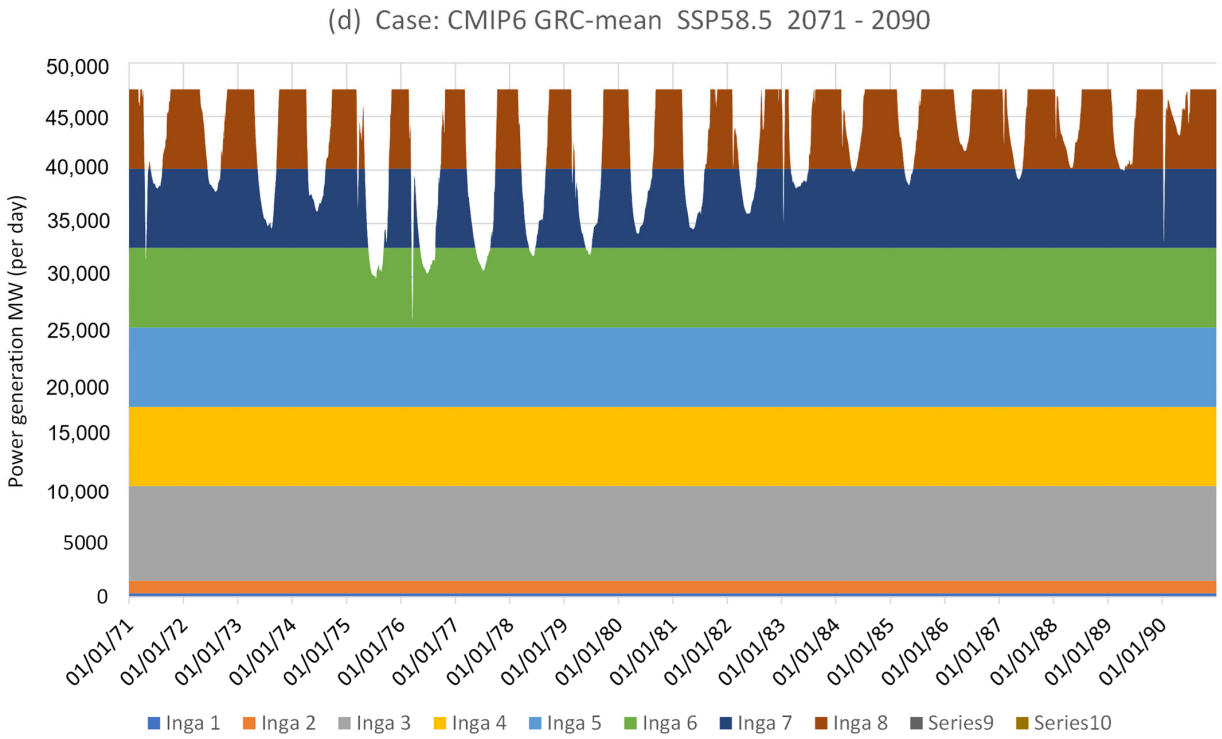

Figure 13. Hydropower generation at Inga Falls for GRC CMIP6 scenarios.

The data suggest that, despite the updated modeling and projections of CMIP6, the overall performance and behavior of hydroelectric production remain remarkably consistent with the previous CMIP5 findings. This alignment between the two sets of scenarios underscores the robustness and reliability of the observations, further reinforcing the implications for hydroelectric production in the context of climate change.

Hydropower Generation from CMIP5 and CMIP6 Scenarios Beyond Inga 8

Downstream from Inga Falls, extending towards the town of Matadi, the river gracefully descends in altitude, covering approximately 38 km with a natural drop ranging from 32 m to 35 m. This residual fall in elevation presents an intriguing prospect for the distant future, particularly when considering advancements in dam construction techniques. It holds the promise of a multifaceted development endeavor that could seamlessly combine the benefits of hydroelectric power generation and enhanced navigability of the river.

This dual-purpose initiative has the potential to not only harness clean energy but also facilitate more efficient transportation and navigation along the waterway. Such a synergy between energy production and navigation could pave the way for a financially viable project, offering a win–win solution for both energy needs and improved river transport.

Figures 14 and 15, as depicted in the graphs, shed light on a pertinent aspect. Under both CMIP5 and CMIP6 scenarios, there appears to be a substantial surplus of water that might otherwise go to waste if not harnessed for power generation purposes, particularly in the context of Inga 9 and 10. This surplus underscores the opportunity for further expansion and development downstream, presenting a compelling case for considering the feasibility of such projects in the broader context of sustainable resource utilization and regional development.

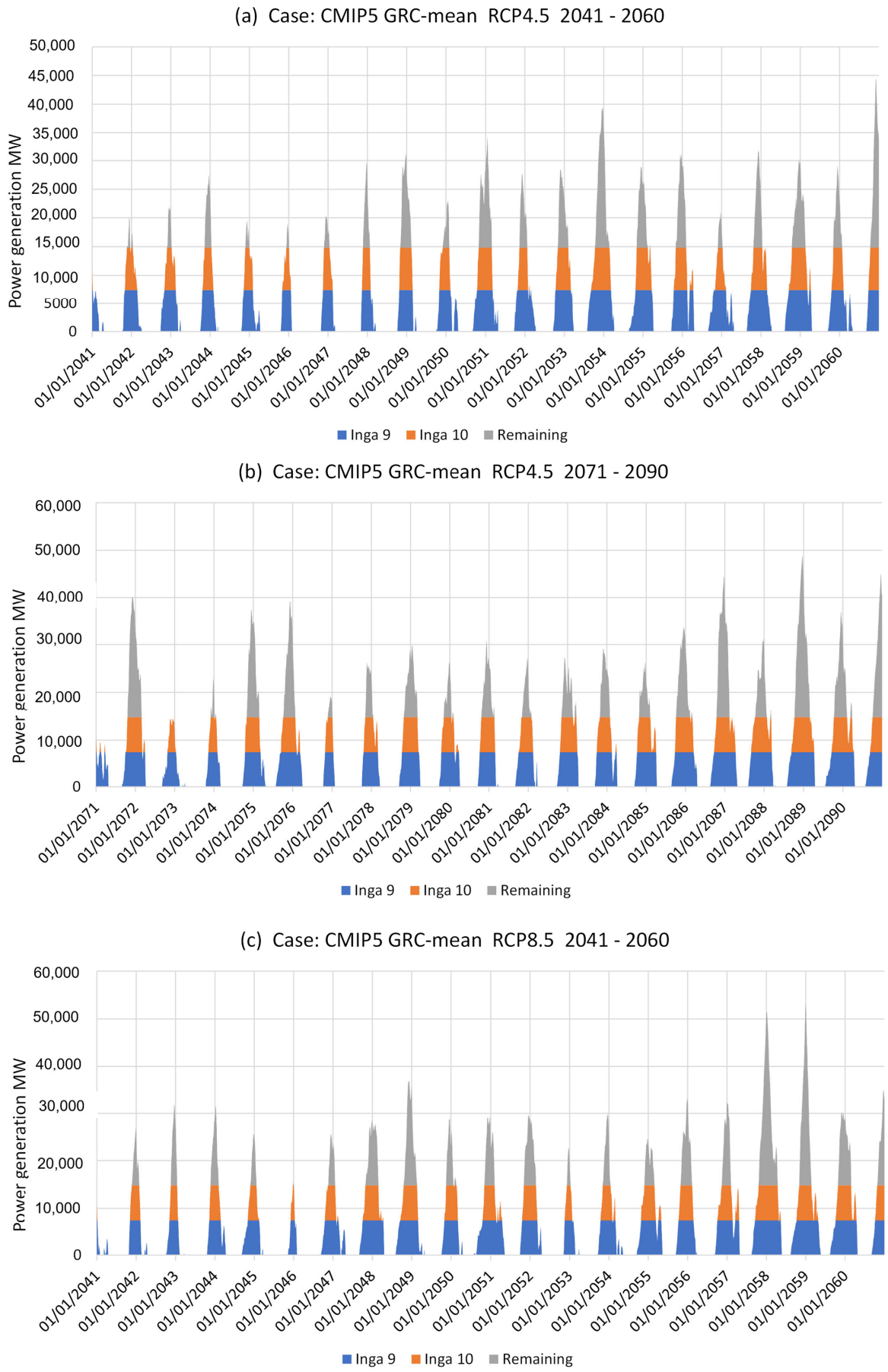

Figure 14. *Cont.*

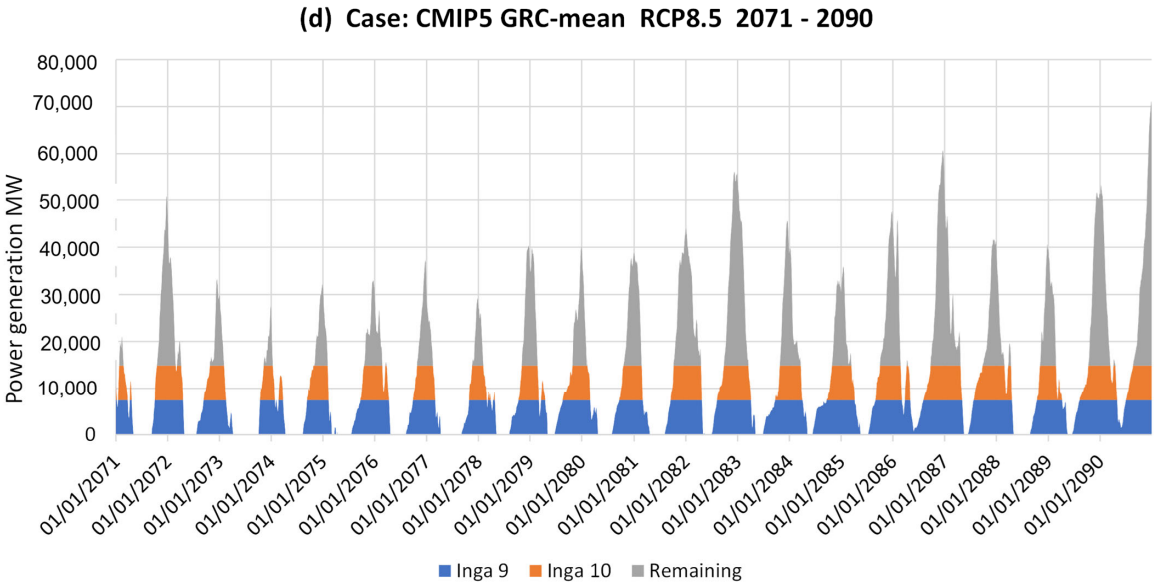

Figure 14. Possible hydropower generation at Inga Falls beyond Inga 8 for GRC CMIP5 scenarios.

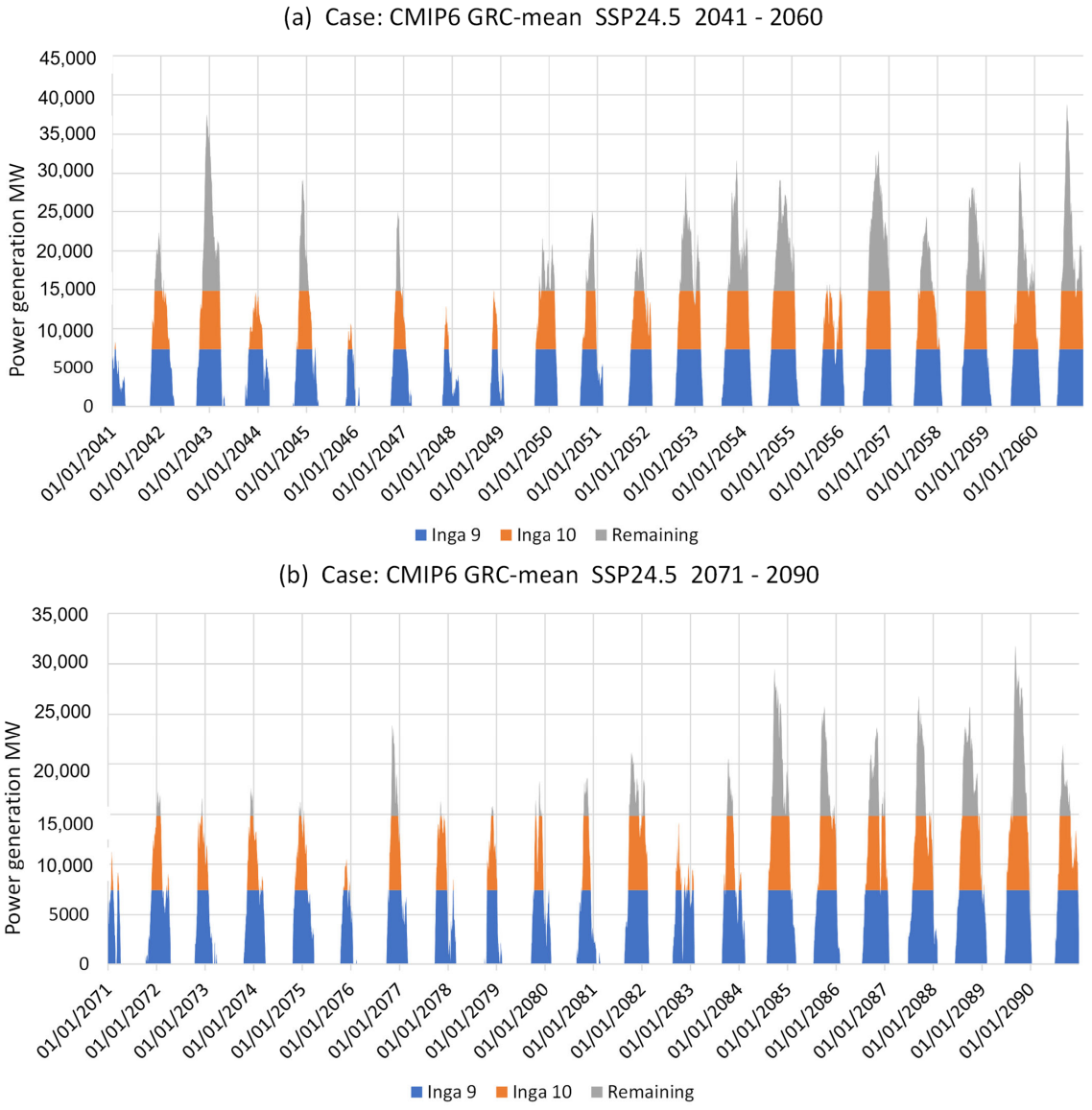

Figure 15. *Cont.*

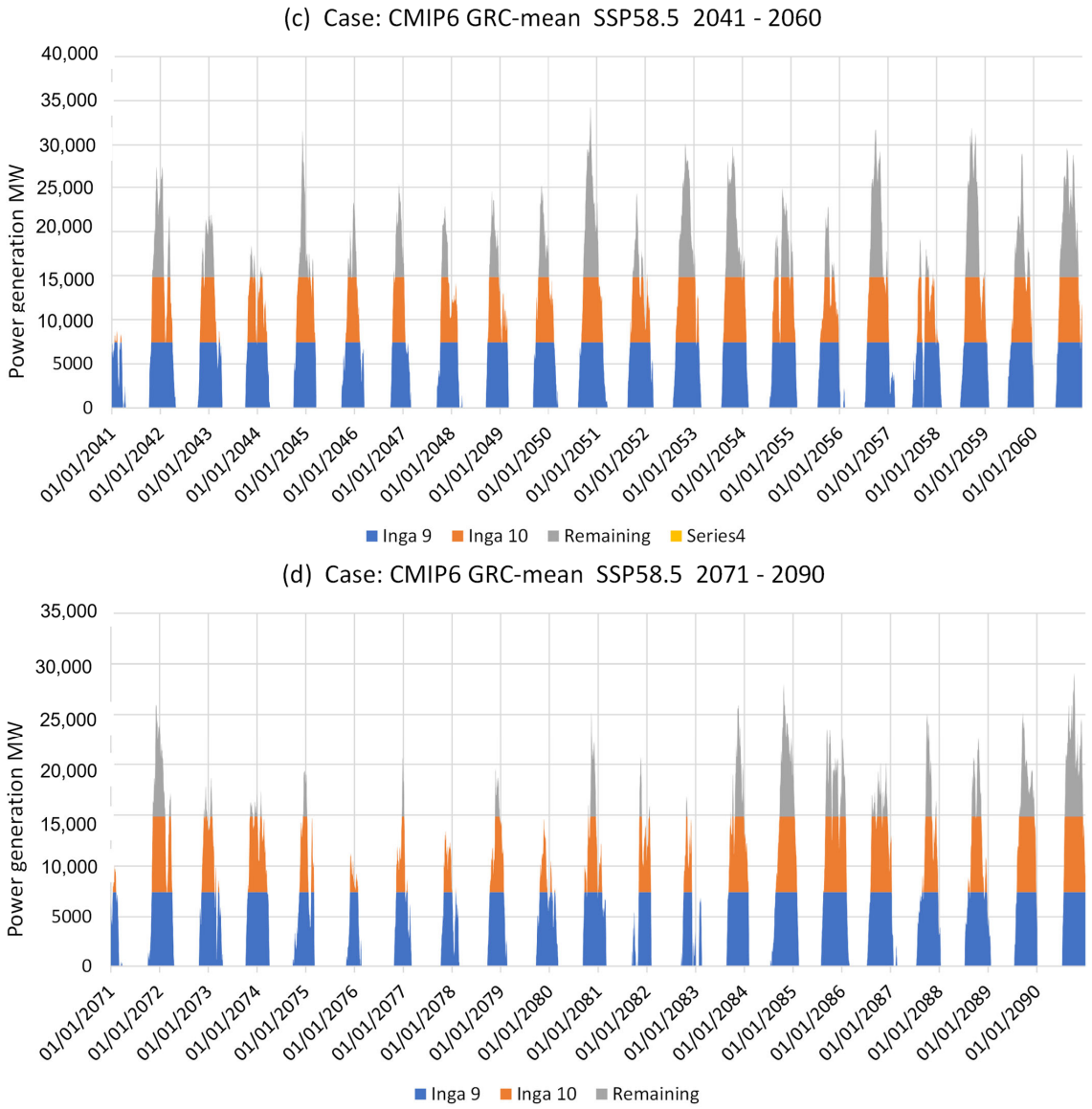

Figure 15. Possible hydropower generation at Inga Falls beyond Inga 8 for GRC CMIP6 scenarios.

5. Conclusions

This research assessed the impact of projected climate change on hydropower generation at the Grand Inga Hydroelectric Project, located on the Congo River in the DRC. This study employed a hydrological model driven by climate projections from 13 NEX-GDDP CMIP6 and CMIP5 datasets under two Representative Concentration Pathways (RCPs) and two Shared Socioeconomic Pathways (SSPs). Using historical streamflow data from the Inga gage, the HEC-HMS hydrological model was calibrated and valiated to simulate the streamflow changes under future climate scenarios. Future periods of analysis included 2041–2060 and 2071–2090, with 1981–2000 as the baseline.

The findings indicate that the technical potential for hydropower generation at Inga Falls is expected to remain robust and even increase under climate change scenarios. Both CMIP5 and CMIP6 datasets suggest that the existing systems (Inga 1 and Inga 2) and planned expansions (Inga 3, 4, and 5) will experience minimal or positive impacts from climate change. However, the later phases of the project (Inga 6, 7, and 8) may face challenges related to increased inter-annual fluctuations in inflows, though these changes are projected to result in an overall increase in generation potential.

These results underscore the importance of adaptive water resources management for the Inga Falls and its upstream basin. To capitalize on potential benefits and mitigate risks associated with increased variability in streamflow, measures such as enhancing flood storage capacity and improving the joint operation of upstream cascade reservoirs are recommended. Such measures can turn potential challenges posed by climate change into opportunities to optimize hydropower generation. Future research should focus on developing integrated water resource management strategies for the upstream basin to ensure the sustainable operation of the Grand Inga Project under changing climatic conditions.

Author Contributions: Conceptualization, S.S.Z. and M.F.; methodology, S.S.Z.; software, Å.K. and S.S.Z.; validation, S.S.Z., Å.K. and M.F.; formal analysis, S.S.Z.; investigation, S.S.Z.; resources, S.S.Z. and M.F.; data curation, S.S.Z.; writing—original draft preparation, S.S.Z.; writing—review and editing, S.S.Z., Å.K. and M.F.; visualization, Å.K. and S.S.Z.; supervision, M.F.; project administration, S.S.Z.; funding acquisition, M.F. All authors have read and agreed to the published version of the manuscript.

Funding: This research received no external funding.

Data Availability Statement: The discharge data that support the findings of this study are available from Régies des voies fluviales (RVF), DR. Congo. Restrictions apply to the availability of these data, which were used under owner permission for this study. These data are available from the authors with the permission of RVF. The meteorological data that support the findings of this study are openly available from the NASA website at https://www.nccs.nasa.gov/services/climate-data-services (accessed on 3 February 2021). The DEM data that support the findings of this study are openly available in SRTM 1 arc second global at https://earthexplorer.usgs.gov/ (accessed on 5 May 2019). The LULC data that support the findings of this study are available at: maps.elie.ucl.ac.be/CCI/viewer/download/ESACCI-LC-Ph2-PUGv2_2.0.pdf (accessed on 3 September 2018). The soil map data that support the findings of this study are available upon request from the FAO website at: https://www.fao.org/soils-portal/data-hub/soil-maps-and-databases/faounesco-soil-map-of-the-world/en/ (accessed on 5 October 2018).

Acknowledgments: We thank Gabriel Mokango from the RVF, DR. Congo, for his help with discharge data.

Conflicts of Interest: The authors declare no conflicts of interest.

References

1. Qin, P.C.; Xu, H.M.; Liu, M.; Du, L.M.; Xiao, C.; Liu, L.L.; Tarroja, B. Climate change impacts on Three Gorges Reservoir impoundment and hydropower generation. *J. Hydrol.* **2020**, *580*, 123922. [CrossRef]
2. Huntington, T.G.; Weiskel, P.K.; Wolock, D.M.; McCabe, G.J. A new indicator framework for quantifying the intensity of the terrestrial water cycle. *J. Hydrol.* **2018**, *559*, 361–372. [CrossRef]
3. Syed, T.H.; Famiglietti, J.S.; Chambers, D.P.; Willis, J.K.; Hilburn, K. Satellite-based global-ocean mass balance estimates of interannual variability and emerging trends in continental freshwater discharge. *Proc. Natl. Acad. Sci. USA* **2010**, *107*, 17916–17921. [CrossRef] [PubMed]
4. Loaiciga, H.A.; Valdes, J.B.; Vogel, R.; Garvey, J.; Schwarz, H. Global warming and the hydrologic cycle. *J. Hydrol.* **1996**, *174*, 83–127. [CrossRef]
5. Cui, T.; Tian, F.Q.; Yang, T.; Wen, J.; Khan, M.Y.A. Development of a comprehensive framework for assessing the impacts of climate change and dam construction on flow regimes. *J. Hydrol.* **2020**, *590*, 125358. [CrossRef]
6. Fluixá-Sanmartín, J.; Altarejos-García, L.; Morales-Torres, A.; Escuder-Bueno, I. Climate change impacts on dam safety. *Nat. Hazards Earth Syst. Sci.* **2018**, *18*, 2471–2488. [CrossRef]
7. van Oorschot, M.; Kleinhans, M.; Buijse, T.; Geerling, G.; Middelkoop, H. Combined effects of climate change and dam construction on riverine ecosystems. *Ecol. Eng.* **2018**, *120*, 329–344.
8. Ehsani, N.; Vörösmarty, C.J.; Fekete, B.M.; Stakhiv, E.Z. Reservoir operations under climate change: Storage capacity options to mitigate risk. *J. Hydrol.* **2017**, *555*, 435–446. [CrossRef]
9. IPCC. *Climate Change 2014–Impacts, Adaptation and Vulnerability: Part A: Global and Sectoral Aspects: Volume 1, Global and Sectoral Aspects: Working Group II Contribution to the IPCC Fifth Assessment Report*; Cambridge University Press: New York, NY, USA, 2014.

10. Berga, L. The Role of Hydropower in Climate Change Mitigation and Adaptation: A Review. *Engineering* **2016**, *2*, 313–318. [CrossRef]
11. Wasti, A.; Ray, P.; Wi, S.; Folch, C.; Ubierna, M.; Karki, P. Climate change and the hydropower sector: A global review. *Wires Clim. Change* **2022**, *13*, e757. [CrossRef]
12. Hamududu, B.; Killingtveit, A. Assessing climate change impacts on global hydropower. In *Climate Change and the Future of Sustainability*; Apple Academic Press: Palm Bay, FL, USA, 2017; pp. 109–132.
13. Lu, S.; Dai, W.; Tang, Y.; Guo, M. A review of the impact of hydropower reservoirs on global climate change. *Sci. Total Environ.* **2020**, *711*, 134996. [CrossRef] [PubMed]
14. Nohara, D.; Kitoh, A.; Hosaka, M.; Oki, T. Impact of climate change on river discharge projected by multimodel ensemble. *J. Hydrometeorol.* **2006**, *7*, 1076–1089.
15. Chilkoti, V.; Bolisetti, T.; Balachandar, R. Climate change impact assessment on hydropower generation using multi-model climate ensemble. *Renew. Energy* **2017**, *109*, 510–517.
16. Turner, S.W.D.; Ng, J.Y.; Galelli, S. Examining global electricity supply vulnerability to climate change using a high-fidelity hydropower dam model. *Sci. Total Environ.* **2017**, *590–591*, 663–675.
17. van Vliet, M.T.H.; Wiberg, D.; Leduc, S.; Riahi, K. Power-generation system vulnerability and adaptation to changes in climate and water resources. *Nat. Clim. Change* **2016**, *6*, 375–380.
18. Zhou, Y.; Hejazi, M.; Smith, S.; Edmonds, J.; Li, H.; Clarke, L.; Calvin, K.; Thomson, A. A comprehensive view of global potential for hydro-generated electricity. *Energy Environ. Sci.* **2015**, *8*, 2622–2633.
19. Liu, L.-L.; Du, J.-J. Documented changes in annual runoff and attribution since the 1950s within selected rivers in China. *Adv. Clim. Change Res.* **2017**, *8*, 37–47. [CrossRef]
20. Liu, L.; Xu, H.; Wang, Y.; Jiang, T. Impacts of 1.5 and 2 °C global warming on water availability and extreme hydrological events in Yiluo and Beijiang River catchments in China. *Clim. Change* **2017**, *145*, 145–158.
21. Schaefli, B. Projecting hydropower production under future climates: A guide for decision-makers and modelers to interpret and design climate change impact assessments. *Wiley Interdiscip. Rev. Water* **2015**, *2*, 271–289.
22. Chen, J.; Brissette, F.P.; Poulin, A.; Leconte, R. Overall uncertainty study of the hydrological impacts of climate change for a Canadian watershed. *Water Resour. Res.* **2011**, *47*, W12509. [CrossRef]
23. Wilby, R.L. Uncertainty in water resource model parameters used for climate change impact assessment. *Hydrol. Process.* **2005**, *19*, 3201–3219.
24. Ludwig, R.; May, I.; Turcotte, R.; Vescovi, L.; Braun, M.; Cyr, J.F.; Fortin, L.G.; Chaumont, D.; Biner, S.; Chartier, I.; et al. The role of hydrological model complexity and uncertainty in climate change impact assessment. *Adv. Geosci.* **2009**, *21*, 63–71.
25. Poulin, A.; Brissette, F.; Leconte, R.; Arsenault, R.; Malo, J.-S. Uncertainty of hydrological modelling in climate change impact studies in a Canadian, snow-dominated river basin. *J. Hydrol.* **2011**, *409*, 626–636.
26. Minville, M.; Brissette, F.; Leconte, R. Impacts and Uncertainty of Climate Change on Water Resource Management of the Peribonka River System (Canada). *J. Water Resour. Plan. Manag.* **2010**, *136*, 376–385.
27. Blöschl, G.; Montanari, A. Climate change impacts—Throwing the dice? *Hydrol. Process. Int. J.* **2010**, *24*, 374–381. [CrossRef]
28. Christensen, N.S.; Lettenmaier, D.P. A multimodel ensemble approach to assessment of climate change impacts on the hydrology and water resources of the Colorado River Basin. *Hydrol. Earth Syst. Sci.* **2007**, *11*, 1417–1434.
29. Kopytkovskiy, M.; Geza, M.; McCray, J.E. Climate-change impacts on water resources and hydropower potential in the Upper Colorado River Basin. *J. Hydrol. Reg. Stud.* **2015**, *3*, 473–493. [CrossRef]
30. Buontempo, C.; Mathison, C.; Jones, R.; Williams, K.; Wang, C.; McSweeney, C. An ensemble climate projection for Africa. *Clim. Dyn.* **2015**, *44*, 2097–2118.
31. Dosio, A.; Panitz, H.-J.; Schubert-Frisius, M.; Lüthi, D. Dynamical downscaling of CMIP5 global circulation models over CORDEX-Africa with COSMO-CLM: Evaluation over the present climate and analysis of the added value. *Clim. Dyn.* **2015**, *44*, 2637–2661.
32. Chen, H.P.; Sun, J.-Q.; Li, H.-X. Future changes in precipitation extremes over China using the NEX-GDDP high-resolution daily downscaled data-set. *Atmos. Ocean. Sci. Lett.* **2017**, *10*, 403–410.
33. Jain, S.; Salunke, P.; Mishra, S.K.; Sahany, S.; Choudhary, N. Advantage of NEX-GDDP over CMIP5 and CORDEX Data: Indian Summer Monsoon. *Atmos. Res.* **2019**, *228*, 152–160.
34. Nzakimuena; St-Pierre, S.; Bossé, Y.; Lorillou, S.; Rousselin, A.; Kitoko, L. Hydroelectric development schemes of the Inga site (Democratic Republic of Congo). In Proceedings of the ICOLD 2013 International Symposium, Seattle, DC, USA, 12–16 August 2013.
35. Zahera, S.S.; Fuamba, M. Grand Inga as One of the Solutions for Africa Energy Deficit. In *Comprehensive Renewable Energy*; Elsevier: Amsterdam, The Netherlands, 2022.
36. Zahera, S.S.; Fuamba, M. 6.21—Grand Inga as One of the Solutions for Africa Energy Deficit. In *Comprehensive Renewable Energy*, 2nd ed.; Letcher, T.M., Ed.; Elsevier: Oxford, UK, 2022; pp. 441–459.

37. Thrasher, B.; Maurer, E.P.; McKellar, C.; Duffy, P.B. Bias correcting climate model simulated daily temperature extremes with quantile mapping. *Hydrol. Earth Syst. Sci.* **2012**, *16*, 3309–3314. [CrossRef]
38. Thrasher, B.; Wang, W.; Michaelis, A.; Melton, F.; Lee, T.; Nemani, R. NASA Global Daily Downscaled Projections, CMIP6. *Sci. Data* **2022**, *9*, 262.
39. Wood, A.W.; Leung, L.R.; Sridhar, V.; Lettenmaier, D. Hydrologic implications of dynamical and statistical approaches to downscaling climate model outputs. *Clim. Change* **2004**, *62*, 189–216.
40. Bhuiyan, H.A.K.M.; McNairn, H.; Powers, J.; Merzouki, A. Application of HEC-HMS in a Cold Region Watershed and Use of RADARSAT-2 Soil Moisture in Initializing the Model. *Hydrology* **2017**, *4*, 9. [CrossRef]
41. Ouédraogo, W.A.A.; Raude, J.M.; Gathenya, J.M. Continuous modeling of the Mkurumudzi River catchment in Kenya using the HEC-HMS conceptual model: Calibration, validation, model performance evaluation and sensitivity analysis. *Hydrology* **2018**, *5*, 44. [CrossRef]
42. Singh; Jain, M.K. Continuous hydrological modeling using soil moisture accounting algorithm in Vamsadhara River basin, India. *J. Water Resour. Hydraul. Eng.* **2015**, *4*, 398–408.
43. Roy, D.; Begam, S.; Ghosh, S.; Jana, S. Calibration and validation of HEC-HMS model for a river basin in Eastern India. *ARPN J. Eng. Appl. Sci.* **2013**, *8*, 40–56.
44. Oudin, L.; Hervieu, F.; Michel, C.; Perrin, C.; Andréassian, V.; Anctil, F.; Loumagne, C. Which potential evapotranspiration input for a lumped rainfall–runoff model?: Part 2—Towards a simple and efficient potential evapotranspiration model for rainfall–runoff modelling. *J. Hydrol.* **2005**, *303*, 290–306.
45. Zelelew, D.G.; Melesse, A.M. Applicability of a Spatially Semi-Distributed Hydrological Model for Watershed Scale Runoff Estimation in Northwest Ethiopia. *Water* **2018**, *10*, 923. [CrossRef]
46. Yuan, W.; Liu, M.; Wan, F. Calculation of critical rainfall for small-watershed flash floods based on the HEC-HMS hydrological model. *Water Resour. Manag.* **2019**, *33*, 2555–2575. [CrossRef]
47. Feldman, A.D. *Hydrologic Modeling System HEC-HMS: Technical Reference Manual*; US Army Corps of Engineers, Hydrologic Engineering Center: Davis, CA, USA, 2000.
48. Tarek; Brissette, F.P.; Arsenault, R. Evaluation of the ERA5 reanalysis as a potential reference dataset for hydrological modelling over North America. *Hydrol. Earth Syst. Sci.* **2020**, *24*, 2527–2544.
49. Arsenault; Brissette, F.; Martel, J.L. The hazards of split-sample validation in hydrological model calibration. *J. Hydrol.* **2018**, *566*, 346–362.
50. Zhang, J.; Hodge, B.-M.; Florita, A.; Lu, S.; Hamann, H.F.; Banunarayanan, V. *Metrics for Evaluating the Accuracy of Solar Power Forecasting*; National Renewable Energy Lab. (NREL): Golden, CO, USA, 2013.
51. Bates, J.M.; Granger, C.W. The combination of forecasts. *J. Oper. Res. Soc.* **1969**, *20*, 451–468.
52. Dickinson, J.P. Some statistical results in the combination of forecasts. *J. Oper. Res. Soc.* **1973**, *24*, 253–260.
53. Dickinson, J.P. Some comments on the combination of forecasts. *J. Oper. Res. Soc.* **1975**, *26*, 205–210. [CrossRef]
54. Newbold, P.; Granger, C.W. Experience with forecasting univariate time series and the combination of forecasts. *J. R. Stat. Soc. Ser. A (Gen.)* **1974**, *137*, 131–146.
55. Arsenault, R.; Essou, G.R.C.; Brissette, F.P. Improving Hydrological Model Simulations with Combined Multi-Input and Multimodel Averaging Frameworks. *J. Hydrol. Eng.* **2017**, *22*, 04016066.
56. Zhang, L.; Yang, X. Applying a multi-model ensemble method for long-term runoff prediction under climate change scenarios for the Yellow River Basin, China. *Water* **2018**, *10*, 301. [CrossRef]
57. Shamseldin, A.Y.; O'Connor, K.M.; Liang, G. Methods for combining the outputs of different rainfall–runoff models. *J. Hydrol.* **1997**, *197*, 203–229.
58. Araghinejad, S.; Azmi, M.; Kholghi, M. Application of artificial neural network ensembles in probabilistic hydrological forecasting. *J. Hydrol.* **2011**, *407*, 94–104.
59. Duan, Q.; Ajami, N.K.; Gao, X.; Sorooshian, S. Multi-model ensemble hydrologic prediction using Bayesian model averaging. *Adv. Water Resour.* **2007**, *30*, 1371–1386.
60. Granger, C.W.J.; Ramanathan, R. Improved Methods of Combining Forecasts. *J. Forecast.* **1984**, *3*, 197–204.
61. Hamududu, B.H. Impacts of Climate Change on Water Resources and Hydropower Systems: In Central and Southern Africa. Ph.D. Thesis, Norges Teknisk-Naturvitenskapelige Universitet, Trondheim, Norway, 2012.
62. Killingtveit, A. *ENMAG User's Manual*; University of Trondheim: Trondheim, Norway, 2004.